A Signature-based Approach to Quantify Soil Moisture Dynamics under Contrasting Land-uses

Ryoko Araki [1], Flora Branger [2], Inge Wiekenkamp (ORCID: https://orcid.org/0000-0003-4800-1160) [3], and Hilary McMillan [1]

[1] Department of Geography, San Diego State University, San Diego, CA

[2] INRAE, UR RiverLy, Centre Lyon-Grenoble Auvergne-Rhône-Alpes, France

[3] Helmholtz Centre Potsdam, GFZ German Research Centre for Geosciences, Germany

Corresponding Author: Ryoko Araki (raraki8159@sdsu.edu)

5500 Campanile Dr, San Diego, CA 92182

Abstract

Soil moisture signatures provide a promising solution to overcome the difficulty of evaluating soil moisture dynamics in hydrologic models. Soil moisture signatures are metrics that quantify the dynamic aspects of soil moisture timeseries and enable process-based model evaluations. To date, soil moisture signatures have been tested only under limited land-use types. In this study, we explore soil moisture signatures' ability to discriminate different dynamics among contrasting land-uses. We applied a set of nine soil moisture signatures to datasets from six in-situ soil moisture networks worldwide. The dataset covered a range of land-use types, including forested and deforested areas, shallow groundwater areas, wetlands, urban areas, grazed areas, and cropland areas. Our set of signatures characterized soil moisture dynamics at three temporal scales: event, season, and a complete timeseries. Statistical assessment of extracted signatures showed that (1) event-based signatures can distinguish different dynamics for all the land-uses, (2) season-based signatures can distinguish different dynamics for some types of land-uses (deforested vs. forested, urban vs. greenspace, and cropped vs. grazed vs. grassland contrasts), (3) timeseries-based signatures can distinguish different dynamics for some types of land-uses (deforested vs. forested, urban vs. greenspace, shallow vs. deep groundwater, wetland vs. non-wetland, and cropped vs. grazed vs. grassland contrasts). Further, we compared signature-based process interpretations against literature knowledge; event-based and timeseries-based signatures generally matched well with previous process understandings from literature, but season-based signatures did

not. This study will be a useful guideline for understanding how catchment-scale soil moisture dynamics in various land-uses can be described using a standardized set of hydrologically relevant metrics.

Keywords: Soil moisture, hydrologic signature, soil moisture signature, land-use, process-based evaluation, metrics-based approach

1. INTRODUCTION

Soil moisture is an important control of water and energy cycles. For example, in rainfall-runoff processes, soil moisture determines the initiation and the response patterns of streamflow (Zehe et al*.,* 2005; Tromp-van Meerveld & McDonnell, 2006; Penna et al., 2011; McMillan & Srinivasan, 2015). In land-atmosphere processes, soil moisture regulates moisture availability in land and atmosphere, and subsequently influences rainfall and evapotranspiration patterns (Eltahir, 1998; Koster & Suarez, 2001; McColl et al., 2019). The role of soil moisture as a modulator between the atmosphere and groundwater storage is explicitly incorporated in many hydrologic models (Singh & Frevert, 2010).

1.1 Scales of soil moisture measurement

Nevertheless, the so-called "scaling problem" often prevents hydrologists from using in-situ soil moisture data for input, calibration, or validation of hydrological models. The scaling problem refers to the mismatch of spatial scales between observations and models. In the field, soil moisture is commonly observed at a point scale by sensors measuring only around the 3-cm vicinity of the installation point (Babaeian et al., 2019). Therefore, the point-scale measurement does not necessarily represent the catchment-scale values, which is often the target scale for hydrologic modeling. Point-scale soil moisture data often contain local variability due to pedology and topography (Vereecken et al., 2016), and such spatially heterogeneous data are sensitive to scaling (Blöschl & Sivapalan, 1995). These scaling issues have discouraged hydrologists from using in-situ soil moisture data for model input or evaluation. However, when evaluated solely based on streamflow dynamics, different hydrologic models can produce similar streamflow responses while producing different soil moisture patterns (Bouaziz et al*.,* 2021). This, in its turn, leads to misrepresentation of soil moisture processes.

This 'scaling problem' has motivated research on representative soil moisture values of a catchment. For example, researchers have intensively studied the best monitoring locations and strategies to capture the soil moisture dynamics (Skøien et al., 2003; De Lannoy et al., 2006; Vereecken et al., 2007; Vanderlinden et al., 2012; Korres et al., 2015; Mälicke et al., 2020). It is becoming common to evaluate modeled soil moisture values or bias-correct the soil moisture values for model input based on the observed mean and variabilities (Draper & Reichle, 2015). However, such statistical metrics do not directly measure the soil moisture dynamics that models aim to reproduce. There remains a need for process-based methods to evaluate soil moisture data, which can be applied to diagnose and transfer soil moisture processes information observed at point scales to model scales.

1.2 Hydrological signature concepts applied to soil moisture

Hydrological signatures have been developed to overcome the difficulty of using hydrologic data in model calibration and evaluation. Hydrological signatures are metrics representing catchment dynamics (Gupta et al., 2008; McMillan, 2020a, 2020b). Hydrological signatures offer a way to identify preferred model structure and parameterization based on the models' ability to reproduce the observed signatures, and therefore the underlying hydrologic processes and dynamics (McMillan, 2020a). Researchers have developed hydrologic signatures to represent various processes, such as streamflow (McDonnell et al., 2007; Yarnell et al., 2015; Gnann et al., 2021a), groundwater (Heudorfer et al., 2019), and snow processes (Schaefli, 2016; Horner et al., 2020), and the impact of environmental alteration on those processes (Richter et al., 1996). When the hydrologic signature concept is applied to analyze soil moisture processes, we call these metrics 'soil moisture signatures.'

1.3 Selecting soil moisture signatures

Soil moisture signatures are designed to quantify soil moisture dynamics at three main temporal scales (Draper & Reichle, 2015; Branger & McMillan, 2020): per storm event ('event-based signatures'), per season ('season-based signatures'), and per a complete time series ('time series-based signatures'). Recent advancements of dense in-situ networks of soil moisture sensors provide soil moisture observation at high spatio-temporal resolution and have enabled the development of various types of signatures. Examples of existing soil moisture signatures include event-based signatures that measure preferential flow occurrence

(Graham & Lin, 2011) and progression of the wetting front (Blume et al., 2009), season-based signatures that measure the persistence of seasonal wet and dry states (Ghannam et al., 2016), and a timeseries-based signature that measures hysteresis in wetting and drying processes (Rosenbaum et al., 2012). Note that these signatures are often mentioned by a different name or are unnamed in literature but are summarized here as 'soil moisture signatures.' Based on individual signatures proposed by these studies, a few studies proposed sets of soil moisture signatures to capture soil moisture dynamics in a standardized manner (Graham & Lin, 2012; Chandler et al., 2017; Branger & McMillan, 2020).

When designing soil moisture signatures, one of the important criteria is discriminatory power: i.e., an ability to discriminate among different soil moisture regimes influenced by relevant physical factors, such as climate, geology, and land-use (McMillan et al., 2017). Fulfilling this criterion allows us to understand and compare soil moisture regimes using signatures. Previous studies have shown that signatures can discriminate between soil moisture dynamics in contrasting climate and geology. Chandler et al. (2017) characterized seasonal wetting, drying, freezing, and melting dynamics in various soil texture types using four timeseries-based signatures for Boise catchments in the United States. Branger & McMillan (2020) explicitly tested the discriminatory power of signatures and found high discriminatory power of season- and timeseries-based signatures among climate classes and among geology classes in New Zealand catchments.

Although land-use is a major determinant of rainfall-runoff and soil moisture processes (Viglione et al., 2016; Rogger et al., 2017; Alaoui et al., 2018), the discriminatory power of signatures between different land-uses has been tested only under limited types of environments. At the same time, previous studies show that describing the discriminatory power of soil moisture signatures is inconclusive. Branger and McMillan (2020) found low discriminatory power of event-based signatures in non-forested and forested areas. Chandler et al. (2017) found low power of timeseries-based signatures to discriminate soil hydraulic characteristics among different tree species. Wiekenkamp et al. (2019), on the other hand, found high discriminatory power of event-based signatures between forested and deforested areas. Some studies found distinct soil moisture values across a wider variety of land-uses, including grazing, cultivation, forests, and grasslands, but their characterizations are limited to spatial mean or variability (Fu et al., 2003; Jawson & Niemann, 2007; Gao et al., 2014; Deng et al., 2016). Testing soil moisture signatures for various land-uses is important for developing a standardized set of signatures that can discriminate the distinct soil moisture processes.

1.4 Aims of this paper

This paper aims to test soil moisture signatures' ability to describe soil moisture dynamics under a range of land-uses. Our work extends the previous studies of soil moisture signatures (Graham & Lin, 2012; Chandler et al., 2017; Branger & McMillan, 2020) by applying their signatures to a wider range of land-uses. The six study sites around the globe are chosen to represent twelve land-use types. All study sites include an internal contrast between two to three land-uses (e.g., deforested vs. forested areas). The paper consists of three sections. The first section reports the impact of data quality on signature calculation (Section 4.1). The second section uses multivariate analysis to evaluate the ability of soil moisture signatures to identify differences in soil moisture dynamics between land-uses (Section 4.2). The third section derives process implications from the differences in signature values between land-uses, by comparing calculated signatures against literature knowledge (Section 4.3).

2. DATA

We analyzed soil moisture data from six networks worldwide under diverse land-uses (Figure 1). We selected soil moisture network sites that have (1) two contrasting land-uses within a network; (2) both soil moisture and rainfall data available at hourly interval; (3) more than two years of data available; (4) catchment scale in size, as larger continental or national scale networks would have large climatic and geologic variation within the network that we sought to avoid. Finally, six sites were chosen to represent twelve types of land-uses from a commonly used land-use and land-cover classification (Anderson et al., 1976; Friedl et al., 2010). For two of the sites, the contrast was in the hydrologic processes (wetland vs. non-wetland in Maqu, and shallow vs. deep groundwater areas in Raam). The site descriptions and sensor configurations are given in Tables 1 and S1, respectively. The soil moisture data were downloaded through the networks' website or obtained from the site manager on request (see Data Availability Section). The soil moisture data were collected using either water content reflectometers, capacitance sensors, or soil dielectric sensors, which respectively calculate the permittivity from the travel time of electromagnetic waves, the change in frequency of electromagnetic waves, or the ratio of reflected voltage. Each observatory used empirical equations suitable for the soil texture to convert the permittivity to the volumetric water content (m^3 of water / m^3 of soil). The original data, whose intervals range from 15 min to 60 min, were aggregated into hourly averages for consistency. We preprocessed soil moisture data for quality control. In most cases, data were preprocessed by each observatory based on its standards. We inspected the remaining errors automatically and manually, as described in Text S1.

We used rainfall datasets either from the soil moisture network station or a nearby weather station (see Data Availability Section and Table S1). The rainfall data were given in a cumulative amount of rainfall (mm) and measured using tipping buckets or weight-based sensors. The original data, whose intervals range from 30 min to 60 min, were aggregated into hourly cumulative amounts (mm/hr) for consistency. If there are multiple rainfall stations at a given site, the one closest to the soil moisture sensors was used for the analysis.

[Insert Figure 1]

[Insert Table 1]

3. METHODS

We tested the discriminatory power of soil moisture signatures to differentiate soil moisture dynamics between land-uses. First, we extracted soil moisture signatures that represent soil moisture dynamics (Section 3.1). Second, we used a multivariate statistic called the Kruskal-Wallis test to compare signature values among land-uses (Section 3.2). Third, we interpreted the process implication of signature differences between land-uses by testing hypotheses built on literature review against the calculated signatures (Section 3.3).

3.1 Soil moisture signatures

As illustrated in Figure 2, we tested nine soil moisture signatures covering three aspects of dynamics (shape, timing, speed) at three temporal scales (per event, per season, and per complete timeseries). The signatures tested are: rising time, normalized amplitude, no-response rate, response type, rising limb density for the event-based signatures; seasonal transition start day and duration for the season-based signatures; distribution type, estimated field capacity, and estimated wilting point for the timeseries-based signatures. All signatures require only soil moisture and rainfall data. The following sections provide detailed descriptions and the algorithm to calculate each signature. The signature definition and the algorithm were based on the original methods, but we adapted them to suit a wide range of soil moisture dynamics and data quality.

[Insert Figure 2]

3.1.1. Event rising time, normalized amplitude, and no-response rate

Event rising time, amplitude, and response rate characterize the runoff dynamics in response to precipitation (Liang et al., 2011; Tian et al., 2019). These signatures were calculated for each storm event. First, following McMillan et al. (2014), rainfall records were divided into events; the start of the event was defined as when the minimum intensity exceeds 2 mm/hr or 10 mm/day after more than 12 hrs of no rainfall; the end of the rainfall was defined as the start of the next rainfall or 5 days after the last rainfall, whichever occurred first. For each event, event rising time was calculated as the time-lag from the start of an event to the soil moisture peak. Event amplitude was calculated as the difference between the soil moisture values at their maximum and at the start of the event, normalized using estimated field capacity and wilting point at the station (defined in Section 3.1.6.) as practiced by Sumargo et al. (2021). Soil moisture was judged as not responding if there was no soil moisture peak detected. In other words, no response of soil moisture means that soil moisture values continued increasing or decreasing during the event. The "no-response rate" was calculated as the number of events with no response divided by the number of all events.

3.1.2. Event response type

We can characterize the flow pathway by comparing the order of response timings along soil profile (Graham & Lin, 2011, 2012; Wiekenkamp et al., 2016a). We applied the methods by Graham and Lin (2011) and Wiekenkamp et al. (2016a) for classifying response types. First, event rising times were calculated as in Section 3.1.1, except that we set the minimum size of response magnitude as 2% of volumetric water content. Then, the response type was classified as 'sequential' when the response order was sequential from the shallow to the deeper sensor. The response type was classified as 'non-sequential' when the order of response times is non-sequential for at least one sensor. 'No-response' was assigned when none of the sensors responded.

3.1.3. Rising limb density

Rising limb density characterizes the catchment flashiness and is often used in streamflow analysis (Sawicz et al., 2011). Rising limb density can also be translated as averaged rising time. We propose rising limb density as a new soil moisture signature that captures the shape of the event rising limbs. We applied an algorithm by Gnann et al. (2021a) for the calculation. First, the rising limb was detected when the rising duration was more than an hour, and the magnitude of change in soil moisture was more than 1% volumetric water content. A 0.01% decrease in volumetric water content during the rising period was allowed. For each rising limb, the length and duration were calculated. Then, rising limb density was calculated as the sum of the rising limb length of all events divided by the sum of the rising time of all events.

3.1.4. Seasonal transition date and duration

Seasonal transition signatures characterize the switching of soil moisture between wet and dry seasons, where different runoff regimes dominate (Grayson et al., 2006). We calculated seasonal transition signatures by fitting a piecewise linear model to the soil moisture timeseries for each wet-to-dry and dry-to-wet transition period. We chose piecewise linear models because the inflection point and plateau can represent the soil moisture value reaching its wetting and drying limit. The seasonal transition was calculated for time series that had bimodal distribution type (defined in Section 3.1.5.) because the signature is only meaningful when soil moisture data show seasonality. First, to remove event-based variability, we aggregated the timeseries from hourly to daily intervals. Then, the wet-to-dry and dry-to-wet transition periods were cropped out. A piecewise linear model was fitted to the cropped time series. Last, the start and end days of the transition were defined as the inflection points of the piecewise linear model, expressed in the day of the year. Transition duration was defined as the length of time between the start and the end day.

3.1.5. Distribution type

Distribution type characterizes the soil moisture storage and seasonality (Rodriguez-Iturbe et al., 1999a, 1999b; D'Odorico et al., 2000; Laio et al., 2001; Samuel et al., 2008). The distribution type was classified based on the number of peaks in the probability density function (PDF) of the soil moisture data. First, we removed trends unrelated to seasonal variability by subtracting the one-year moving mean from the time series as practiced by Basak et al. (2017). Second, the soil moisture PDF was obtained using Kernel smoothing with twice the optimal bandwidth, which is optimal to represent PDF by normal distributions. Third, PDF peaks were detected if a given data sample point was larger than the two neighboring data samples. Peaks with a magnitude smaller than 20% of the largest peak were eliminated. We used MATLAB Signal Processing Toolbox for peak detection. Last, PDFs were classified according to the number of peaks into "unimodal" (one peak), "bimodal" (two peaks), or "multimodal" (three or more peaks).

3.1.6. Estimated field capacity and wilting point

Soil moisture timeseries often exhibit seasonal wet and dry equilibriums, which represent the water holding capacity of the soil. Since the values are known to be comparable to field capacity and wilting point estimated from soil core sample experiments (Chandler et al., 2017; Bean et al., 2018), we define them in this paper as 'estimated' field capacity and wilting point. We calculated the estimated field capacity and wilting point as the peaks of the soil moisture PDF. First, peaks of the soil moisture PDF were detected as in Section 3.1.5. The peak with the largest and smallest volumetric soil moisture content was defined as the estimated field capacity and wilting point, respectively. If the estimated field capacity and wilting point coincided (i.e., distribution type was unimodal), both values were discarded. In this way, we automated the calculation of estimated field capacity and wilting point, which is commonly done by manually labeling the wet and dry equilibrium values in the timeseries.

3.2 Statistical assessments

After calculating the signatures described in Section 3.1, we compared signature differences between land-uses using statistical tests. The statistical significances represent the discriminatory power of signatures to distinguish differences in dynamics across land-uses; in other words, the differences in dynamics outweigh the overall data uncertainty. A comparison was made between two or three contrasting land-uses within each study site (i.e., in total, six land-use comparisons for six study sites). As climate and geology will be strong confounding factors, comparison across all study sites was not implemented. For most signatures, we used the non-parametric Kruskal-Wallis test (Kruskal & Wallis, 1952). The Kruskal-Wallis test is a non-parametric method to test whether the data originate from identical distributions based on ranks. Non-parametric tests were chosen because soil moisture signatures often show skewed distributions (Branger & McMillan, 2020). We interpreted the difference as significant when the p-value is less than 0.05. The Kruskal-Wallis test was applied to signatures in interval or ratio form (all signatures except response type and distribution type). The Kruskal-Wallis test was not applicable for categorical variables, so we took a different approach for such signatures (response type and distribution type signatures). We calculated the 'dominance' of one category: the ratio of the number of samples in one category (sequential for response type; unimodal for distribution type) to the total number of samples (which is equal to the sum of sequential and non-sequential responses for response type; the sum of unimodal, bimodal, and multimodal distribution for distribution type). We used the change in the 'dominance' ratio of one category to measure differences between the two groups.

3.3. Process interpretation

We took a hypothesis-testing approach to understand how signature values relate to soil moisture processes (McKnight, 2017; Gnann et al., 2021b). First, we explored the interpretation of signature values based on expert knowledge in literature. We reviewed two types of literature: articles about the study site of interest, and articles about a watershed with a similar hydrologic environment to the study site of interest that investigated the processes using a signature-based approach on their soil moisture data. To build the overarching interpretation of signature values, we focused on catchment functionality. According to Black (1997) and Wagener et al. (2007), catchment functionality consists of four basic elements: partition, transmission, storage, and release. Among them, two functionalities are closely related to the soil moisture system: partitioning that corresponds to flow pathways of rainfall in soil or at the soil surface, and storage that corresponds to the amount of water stored in the soil. After building an overarching interpretation focused on these two functionalities, we tested them against the signature values from the soil moisture networks. We refined or updated our hypotheses if the signature differences were not satisfactorily explained.

4. RESULTS

4.1 Data quality assessment and its impact on signature extraction

This section demonstrates the data quality and its impact on our research design. The results of the data quality assessment show that sufficient data were obtained for statistical assessments. Kruskal-Wallis test requires a sample size of five or more to determine statistical significance (Riffenburgh, 2006). In Figure 3, the number of reliable timeseries exceeds five for most of the study sites. When there were less than five reliable stations within a testing group (consisting of a combination of a depth and a land-use), we could not complete the statistical assessment, especially for signatures that can be only extracted once per time series (estimated field capacity, estimated wilting point, no-response rate, and rising limb density signatures). Other signatures were robust to the lack of reliable data as they can be extracted once per season (seasonal transition date and duration) or event (event rising time, response type, amplitude).

[Insert Figure 3]

Overall, signature values showed clear differences among the study sites (Figure 4). This implies that the signatures were successfully extracted and can be used for further analysis. Signature differences between study sites can be attributed to the differences in their climate and geology. For example, estimated field capacity was clearly correlated with aridity index, except for Maqu (MQ), where wetland areas produced unusually organic-rich soil. However, analysis of climate and geology controls on signature values is beyond our scope and not further discussed.

[Insert Figure 4]

4.2 Signature differences between contrasting land-uses

This section provides an overview of how soil moisture signature values change depending on the land-use. We explain signature differences between land-uses from two perspectives: the magnitude (whether the signature magnitude for a given soil depth differs between land-uses) and the profile along soil depth (whether the increasing or decreasing trend of signature values relative to soil depth differs between land-uses). Figures 5 and S1 show the signature differences in terms of the magnitude and the profile, respectively. Figures 6, 7, and 8 show the boxplots of selected signatures that showed notable differences between land-uses. Please refer to the supplemental material for boxplots of signature values for all the study sites (Figures S2, S3, and S4).

Interpretation of Figure 5 is as follows. In Figure 5, signatures that were statistically significantly different between land-uses are highlighted in darker blue. For example, many cells in the column of "event-based signatures" are highlighted in darker blue in Figure 5, indicating that event-based signatures showed a high ability to distinguish different dynamics between the study sites (called 'discriminatory power' hereafter). The arrows in the cells help understand the direction of change in signature values. For example, the up-pointing arrow for amplitude signature in Wüstebach (WB) means the event amplitudes were larger in the deforested area than the forested area.

Overall, event-based signatures showed high discriminatory power between contrasting land-uses for all sites. Season- and timeseries-based signatures showed moderate discriminatory power in deforested, urban, shallow groundwater, and croplands. Signature differences between land-uses were observed both in terms of their magnitude and profile. The following subsections describe the detailed results by signature timescale (event-, season-, and timeseries-based signatures).

[Insert Figure 5]

4.2.1. Event-based signatures

Event-based signatures showed differences between land-uses both in magnitude and in signature profile with soil depth. Differences in signature values were found across most land uses, with notable differences between deforested vs. forested and urban vs. greenspace contrasts.

Figure 5 shows that event-based signatures varied in magnitude with land-use for all study sites; in Figure 5, cells are highlighted in darker blue for statistically significant signatures. Statistically significant differences were found for amplitude and rising time signatures at all sites, and for rising limb density and "no-response rate" signatures at Wüstebach. These changes in signature magnitudes indicate a more responsive regime especially in the deforested area than the forested area at Wüstebach, and the shallow groundwater area than the deep groundwater area at Raam.

Figure 6 shows examples of how event-based signature profiles with soil depth changed between land-uses in Wüstebach (deforested vs. forested) and Hamburg (urban vs. greenspace). In Wüstebach, rising limb density increases with depth in the forested area, whereas the values were similar with soil depths in the deforested area (Figure 6a). In Hamburg, the event-based signatures were more pronounced at the shallow depth (sensors at 5 and 20 cm depths) in the urban area than in the greenspace (Figure 6b, c, d).

We interpret the changes in event-based signatures to represent the influences of wetness conditions on the storage processes and the influences of soil properties on the flow partitioning process (see Section 4.3.1).

[Insert Figure 6]

4.2.2. Season-based signatures

Season-based signatures showed differences in magnitude and in profile with soil depth for some types of land-uses, namely, deforested vs. forested, urban vs. greenspace, and cropland vs. grazed vs. grassland contrasts.

Figure 5 shows that season-based signature values varied in magnitude with land-use in Wüstebach (deforested vs. forested), Hamburg (urban vs. greenspace), and Oznet (crop vs. grazed vs. grassland); in Figure 5, cells are highlighted in darker blue for statistically significant signatures. In Wüstebach, the wet season persisted longer in the deforested area than in the forested area; the dry-to-wet transition started earlier and took a shorter time, and the wet-to-dry transition duration took a longer time. In Hamburg, wetting up was more gradual, and drying out was more rapid in the urban area than in the greenspace.

Figure 7 shows that season-based signature profiles with soil depth changed between land-uses in Wüstebach (deforested vs. forested) and Oznet (crop vs. grazed vs. grassland). In most sites, the seasonal transition propagated from shallow to deep soil layer, or occurred in tandem at all depths. On the contrary, the transition started earliest in the deeper layer in the deforested area in Wüstebach (Figure 7a) and cropland in Oznet (Figure 7b and c). We interpret the changes in season-based signatures to represent the influences of water balance and soil wetness conditions on storage processes (see Section 4.3.2).

[Insert Figure 7]

4.2.3. Timeseries-based signatures

Timeseries-based signatures showed differences in magnitude and in profile with soil depth for most types of land-uses, namely, deforested vs. forested, wetland vs. non-wetland, shallow vs. deep groundwater, and cropped vs. grazed vs. grassland contrasts.

Figure 5 shows that timeseries-based signature values varied in magnitude with land-use; changes in estimated field capacity and wilting point were statistically significant in Wüstebach (deforested vs. forested), and changes in the dominance of unimodal distribution type were more than 15% in most of the study sites except Texas (grazed vs. ungrazed). Not statistically significant due to small sample sizes, but visual differences in the signature magnitude were seen in Maqu (wetland vs. non-wetland) for estimated field capacity (Figure 8a) and Oznet (crop vs. grazed vs. grassland) for estimated wilting point (Figure 8b). These changes in signature magnitude imply wetter conditions in the deforested area in Wüstebach, wetlands in Maqu, and grasslands in Oznet.

Figure 8 shows the timeseries-based signature profiles with soil depth changed between land-uses in Hamburg (urban vs. greenspace) and Raam (shallow vs. deep groundwater). In Hamburg, variability of estimated field capacity and wilting point decreased with depth in the greenspace, whereas they increased in the urban area (Figure 8c). In the shallow groundwater area of Raam, the bimodal distribution is dominant at the deepest and shallowest soil, contrasting to mixed modality along all depths in the deep groundwater area (Figure 8d). We interpret that the changes in timeseries-based signatures represent the influences of soil properties, vegetation, and groundwater on the storage processes (see Section 4.3.3).

[Insert Figure 8]

4.3. Interpretation of signature differences between land-uses

This section provides interpretations of the signature difference among contrasting land-uses derived in Section 4.2. Figure 9 shows whether the observed signature differences between land-uses agreed with literature interpretations. Overall, event-based and timeseries-based signatures mostly agreed (cells are highlighted blue in Figure 9), whereas season-based signatures poorly agreed with literature (highlighted red in Figure 9). The following sections describe the detailed results by signature timescale (event-, season-, and timeseries-based signatures).

[Insert Figure 9]

4.3.1. Event-based signatures represent partitioning processes

In general, event-based signatures matched with expert knowledge in literature (highlighted blue in Figure 9). Event-based signature differences in magnitude represented changes in storage flashness, and those in the signature profile represent changes in flow partitioning processes depending on the land-uses.

We interpreted the event-based signature magnitudes between land-uses to represent the storage flashiness depending on the soil wetness conditions. Larger response amplitude, shorter rising time, larger rising limb density, and lower "no-response rate" imply flashier storage response in high soil wetness conditions. Our signatures showed greater storage flashiness in deforested areas (Wüstebach) and cropped areas (Oznet). These land disturbances are known to increase soil wetness (and therefore flashiness) through reduced transpiration and interception (Wiekenkamp et al., 2016b) and irrigation (Smith et al., 2012), respectively. Response amplitude gets smaller when the soil wetness is close to saturation (Soylu & Bras, 2021). We observed this change in Raam (shallow vs. deep groundwater) and Maqu (wetland vs. non-wetland).

We interpreted that the changes in the event-based signature profiles imply changes in flow partitioning processes. According to Graham and Lin (2011), sequential responses ordering from shallow to deep soil layer represent vertical infiltration and overland flow regime, and non-sequential response patterns (random response order along soil depth) represent preferential or lateral flow regime. Additionally, more pronounced responses in shallow soils within sequential-response patterns represent the overland flow regime (Ziegler et al., 2001).

Our signature values agreed with this interpretation; we saw sequential and more pronounced responses in shallow soil in urban areas in Hamburg and cropped areas in Oznet, where surface sealing (Scalenghe & Ajmone-Marsan, 2009) and compaction (Alaoui et al., 2018) are expected to increase overland flow, respectively. A decrease in non-sequential response was found in Wüstebach, where preferential flow is known to decrease after deforestation (Wiekenkamp et al., 2019). On the other hand, event-based signatures did not show significant changes in grazed vs. ungrazed areas in Texas (Alaoui et al., 2018), contrary to the expectation that compaction increases overland flow at this site. This might be due to scale, as plot-scale compaction does not always influence catchment-scale response (Rogger et al., 2017; Alaoui et al., 2018).

4.3.2. Season-based signatures represent storage processes

Season-based signatures only partially matched with expert knowledge in literature (highlighted blue for a match, red for no match in Figure 9). We interpret that a combination of the following factors related to storage processes affects season-based signatures' magnitude and profile: changes in water balance depending on the active root depth and rainfall rate (Laio, 2002), the closeness of soil wetness conditions to soil moisture threshold (Detty & McGuire, 2010), and other land-use influences such as groundwater (Miguez-Macho & Fan, 2012), construction waste (Wiesner et al., 2016), and irrigation (Smith et al., 2012). For example, reduced rainfall rate and root depth explained earlier transition start date, and higher wetness conditions explained shorter transition duration in the shallow soil layer in deforested vs. forested contrast in Wüstebach; still, literature did not fully explain the changes of the signature profile along soil depth. The mismatch was more obvious in land-uses that complicate the boundary conditions of soil water storage, such as construction waste presence in the soil in Hamburg or strong groundwater influence in Raam (highlighted red in Figure 9). The mismatch can also be attributed to a lack of studies on season-based signatures. Many studies on soil moisture seasonality mainly concentrate on detecting anomalies for drought analysis or general trends for land-surface process understandings (Koster & Suarez, 2001; Kumar et al., 2019; Potter et al., 2005; Teuling et al., 2005). In contrast, few studies exist on the influence of land-use on soil moisture seasonal transition timings and durations.

4.3.3. Timeseries-based signatures represent storage characteristics

In general, the timeseries-based signature matched with expert knowledge in literature (highlighted blue in Figure 9). Changes in timeseries signatures represented the interaction between soil water storage and soil properties, vegetation, and groundwater depending on the land-uses.

We interpreted the timeseries-based signature magnitudes to represent the amount of soil water storage. Larger estimated field capacity, wilting point, and dominance of unimodality imply more soil water stored. Signature values matched literature expectations in Wüstebach (deforested vs. forested), Maqu (wetland vs. non-wetland), and Oznet (crop vs. grazed vs. grassland), where deforested, wetland, and cropped conditions are respectively known to increase soil wetness through changes in transpiration (Wiekenkamp et al., 2016b), soil organic content (Dente et al., 2012; Hudson et al., 1994), and irrigation (Smith et al., 2012).

We interpreted that the changes in the timeseries-based signature profile with soil depth imply the external influence on soil water storage. Generally, the estimated field capacity and wilting point either consistently decrease or increase with soil depth, and the dominance of unimodal distribution increases with soil depth, because of less influence of climate and compaction of pore spaces in the deeper soil (Trimble, 2007). Different behavior seen in the shallow groundwater area at Raam can be explained as follows; at the groundwater interface, the saturation is controlled by whether the groundwater meets the soil sensors or not, and bimodal distribution becomes dominant again. High variability of estimated field capacity and wilting point in deeper soil in urban areas in Hamburg can be explained by the urban structures or construction waste that creates different sizes of pores (Wiesner et al., 2016).

5. DISCUSSION

5.1. Limitations

We recognize several limitations in our study. First, future work should test differences in signature values attributed to land-use against confounding factors. For example, we explicitly examined groundwater influence for Raam, but groundwater could also influence soil moisture dynamics in Wüstebach, Hamburg, and Maqu. Such confounding factors include topography, slope aspects, position in slope, snow influence, distances between sensors, and sensor types. However, investigation on confounding factors requires detailed datasets on elevation, groundwater depth, snow depth, or temperature at each sensor location, which are not consistently available for all the study sites. We treated the contrasting land-use as the major controls on soil moisture processes and took variability of other factors within a catchment as residual uncertainty in this study (Beven, 2000). Our selection of sites, where sensors are within watershed-scale, helps reduce the impact of the confounding factors. For confounding factors regarding soil moisture network design (e.g., size of the network and distance between sensors), it would be beneficial to implement geospatial analysis. Previous studies suggest that investigating the influence of spatial scale on soil moisture values advances our understanding of the soil moisture processes (Brocca et al., 2007; Gómez-Plaza et al., 2001; Western et al., 2004).

Second, the signature approach needs attention when adapted to different hydrologic environments. We encountered several difficulties in extracting and interpreting signatures under different climate and soil conditions (e.g., defining seasonal transition for sites with an unstable wet season, multiple process interpretations for bimodal distribution signatures, and the impact of data quality practice on signature calculation). We summarized our experiences and recommendations in Text S2. Also, our datasets did not cover some combinations of land-use and climates. For example, grazed land-use was tested only in Texas and Oznet under an arid climate, not in humid and temperate climates. Therefore, the users should be careful using signatures on other climates, soil types, or soil developments. Future work should fill the gaps using larger datasets, such as the International Soil Moisture Network dataset (Dorigo et al., 2011) or SMAP satellite observation (Entekhabi et al., 2014).

5.2. Novelty, usefulness, and future direction of soil moisture signature approach

There are two novelties of this study. First, this study showed clear differences in soil moisture signatures depending on land-uses. Previous studies compared signatures under limited land-uses (e.g., forest vs. non-forest in Branger & McMillan, 2019; forests with various tree species in Chandler et al., 2017). Previous studies also compared signatures from the large-scale observation networks, where climate and geology are the strong confounding factors. This study covered a wide range of land-uses and conducted internal comparisons within small to mesoscale observation networks. The research design allowed analyses with a strong focus on land-use impacts on signature values, and interpretation of the signature values based on catchment-scale processes. Second, this study differentiated soil moisture processes between land-uses only using soil moisture and rainfall datasets. Usually, watershed processes are understood using a variety of hydrological and soil observations. However, rich process knowledge from previous studies allowed us to interpret processes from signature values calculated only from soil moisture and rainfall data. Using standardized metrics, the process interpretation across study sites also helped integrate individual knowledge of existing soil moisture studies.

Our results suggest potential uses of soil moisture signatures in hydrologic analysis to represent the different dynamics with land-uses. In the future, hydrologists could use soil moisture signatures to calibrate, constrain, or evaluate models against observation data, as practiced in streamflow signatures (Westerberg et al., 2011; Shafii & Tolson, 2015). Models could be evaluated whether the model represented significant differences or similarities in soil moisture signature values expected between different land-uses. Signatures could also be used to compare satellite data against in-situ data in terms of soil moisture dynamics. Our results imply that significant differences in signature values between land-uses appear even at 5 cm soil depth, which is a typical penetration depth of remote sensing observation. Furthermore, signatures could be used for process investigation or model structure identification between contrasting land-uses especially for the event- and the timseries-based signatures, whose process implications were successfully derived in this study. Signatures would be especially useful to represent different dynamics for the land-use contrasts that showed significant signature differences (deforested vs. forested, urban vs. greenspace, crop vs. grazed vs. grassland).

Ultimately, we would like to develop a systematic classification of catchment processes between land-uses based on signatures (Wagener et al., 2007). As an example, we designed a flow chart to show how partitioning processes might be classified using event-based signatures (Figure 10). First, the flow pathways could be categorized into sequential and non-sequential types based on response type signatures, and then further refined based on other event-based signatures. Several signatures are lacking (in grey letters in Figure 10), but this flow chart demonstrates the potential of a signature-based process classification system. For example, the flow chart represents the signature difference in urban vs. greenspace area between vertical vs. overland flow processes, which we observed in Hamburg. Previous studies have suggested promising classification frameworks for soil moisture processes. For example, Boorman et al. (1995) propose eleven basic modes for partitioning processes depending on the soil profile and groundwater position, and Grayson et al. (1997) propose four basic modes for storage seasonality depending on the soil wetness conditions. We could potentially classify catchment processes using soil moisture signatures at all temporal scales based on these studies.

[Insert Figure 10]

6. CONCLUSIONS

Soil moisture signatures are metrics that represent soil moisture dynamics. This study aimed to test soil moisture signatures' ability to discriminate different dynamics under contrasting land-uses (called 'discriminatory power'). We integrated nine soil moisture signatures from previous studies (Branger & McMillan, 2020; Graham & Lin, 2012; Chandler et al., 2017; Sawicz et al., 2011). The set of signatures quantified the dynamics at three temporal scales: event, season, and complete timeseries. We applied the signatures to six soil moisture network data with diverse land-uses, including deforested, shallow groundwater, wetlands, urban, grazed, and cropland areas. Using statistical, visual, and literature analysis, we tested the discriminatory power of soil moisture signatures.

Event-based signatures had the highest discriminatory power; they showed clear statistical and visual differences across all land-uses. Literature supported the link between partitioning and storage processes, and event-based signatures. Season-based signatures had moderate discriminatory power; they showed statistical and visual differences in a range of land-uses (e.g., deforested vs. forested, urban vs. greenspace, crop vs. grazed vs. grassland). However, literature could not fully explain the differences in season-based signatures depending on the land-uses due to the lack of observational studies using the season-based signature approach. Timeseries-based signatures had moderate discriminatory power in all land-uses except in grazed vs. ungrazed. The differences of timeseries-based signatures between land-uses were linked to differences in storage characteristics.

Our results demonstrated that soil moisture signatures, calculated only from soil moisture and rainfall timeseries, can capture the land-use impacts on catchment-scale soil moisture dynamics. We also explored and documented the limitation in extracting signatures from datasets covering a wide range of climate conditions. This study will be a useful guideline for hydrologists to apply soil moisture signatures for evaluating land-use impacts on hydrologic processes and developing a standardized classification system of soil moisture processes.

ACKNOWLEDGEMENTS

We thank Dr. Heye Bogena, Dr. Sarah Wiesner and Dr. Ingo Lange, Dr. Harm Jan Frederik Benninga, Dr. Bongiovanni Tara, Dr. Bob Su, Dr. Laura Dente, Dr. Jeffrey Walker, and Dr. Mei Sun Yee for providing data and site information. We thank Dr. Trent Biggs, Dr. Alicia Kinoshita, Dr. Takahiro Sayama, and Dr. Sebastian Gnann for helpful discussions. Last but not least, we are grateful to the editor and two anonymous reviewers for their thoughtful comments on this manuscript.

DATA AVAILABILITY

The datasets used in this study are available from the following. Please visit the observatory's website or inquire the site manager for the availability of data.

Study sites	Soil moisture data source	Rainfall data source
Wüstebach (WB)	Requested to Dr. Heye Bogena (h.bogena@fz-juelich.de) Note that data through 2009 to 2015 are available online (Bogena, 2021)	Online. Used Monschau-Kalterherberg station data (The Deutscher Wetterdienst (DWD), 2021)
Hamburg (HB)	Requested to Dr. Sarah Wiesner (sarah.wiesner@uni-hamburg.de) Network description is available online (University of Hamburg, 2021)	Online. Used Hamburg-Fuhlsbüttel station data (The Deutscher Wetterdienst (DWD), 2021)
Raam (RM)	Online. 2016-2017 data (Benninga et al., 2017) 2017 -2018 data (Benninga et al., 2018a) 2018 – 2019 data (Benninga et al., 2020)	Online. Used Volkel weather station data (The Royal Netherlands Meteorological Institute (KNMI), 2021)
Texas (TX)	Online (Bongiovanni & Caldwell, 2019)	Online (Bongiovanni & Caldwell, 2019)

Maqu (MQ)	Requested to Dr. Bob Su (z.su@utwente.nl) 5 cm sensor data is available online (Dorigo et al., 2011)	Requested to Dr. Bob Su (z.su@utwente.nl)
Oznet (OZ)	Online (Smith et al., 2012)	Online (Smith et al., 2012)

REFERENCES

Alaoui A, Rogger M, Peth S, Blöschl G. 2018. Does soil compaction increase floods? A review. *Journal of Hydrology* **557**: 631–642 DOI: 10.1016/j.jhydrol.2017.12.052

Anderson JR, Hardy EE, Roach JT, Witmer RE. 1976. A Land Use and Land Cover Classification System for Use with Remote Sensor Data. U.S. Geological Survey Professional Paper **964**, p. 28.

Babaeian E, Sadeghi M, Jones SB, Montzka C, Vereecken H, Tuller M. 2019. Ground, Proximal, and Satellite Remote Sensing of Soil Moisture. *Reviews of geophysics* **57** (2): 530–616 DOI: 10.1029/2018RG000618

Basak A, Mengshoel OJ, Kulkarni C, Schmidt K, Shastry P, Rapeta R. 2017. Optimizing the decomposition of time series using evolutionary algorithms: soil moisture analytics. In *Proceedings of the Genetic and Evolutionary Computation Conference* Association for Computing Machinery: New York, NY, USA; 1073–1080 DOI: 10.1145/3071178.3071191

Bean EZ, Huffaker RG, Migliaccio KW. 2018. Estimating Field Capacity from Volumetric Soil Water Content Time Series Using Automated Processing Algorithms. *Vadose Zone Journal* **17** (1): 180073–180073 DOI: 10.2136/vzj2018.04.0073

Benninga HF, Carranza CD, Michiel-Pezij MJ, van der Ploeg DCM, Augustijn R, van der Velde R. 2017. Regional soil moisture monitoring network in the Raam catchment in the Netherlands - 2016-04 / 2017-04 [version 1] DOI: 10.4121/UUID:DC364E97-D44A-403F-82A7-121902DEEB56

Benninga HF, Carranza CD, Michiel-Pezij MJ, van der Ploeg DCM, Augustijn R, van der Velde R. 2018a. Regional soil moisture monitoring network in the Raam catchment in the Netherlands - 2017-04 / 2018-04 DOI: 10.4121/UUID:AFB36AC8-E266-4968-8F76-0D1F6988E23D

Benninga HF, Carranza CD, Michiel-Pezij MJ, van der Ploeg DCM, Augustijn R, van der Velde R. 2020. Regional soil moisture monitoring network in the Raam catchment in the Netherlands - 2018-04 / 2019-04 DOI: 10.4121/UUID:B68E3971-C73E-4D7F-B52F-9EF7D7FE1ED2

Benninga HJF, Carranza CDU, Pezij M, Van Santen P, Van Der Ploeg MJ, Augustijn DCM, Van Der Velde R. 2018b. The Raam regional soil moisture monitoring network in the Netherlands. *Earth System Science Data* **10** (1): 61–79 DOI: 10.5194/essd-10-61-2018

Beven KJ. 2000. Uniqueness of place and process representations in hydrological modelling. *Hydrology and Earth System Sciences* **4** (2): 203–213 DOI: 10.5194/hess-4-203-2000

Black PE. 1997. Watershed functions. *Journal of the American Water Resources Association* **33** (1): 1–11 DOI: 10.1111/j.1752-1688.1997.tb04077.x

Blöschl G, Sivapalan M. 1995. Scale issues in hydrological modelling: A review. *Hydrological processes* **9** (3–4): 251–290 DOI: 10.1002/hyp.3360090305

Blume T, Krause S, Meinikmann K, Lewandowski J, Zehe E, Bronstert A. 2009. Use of soil moisture dynamics and patterns at different spatio-temporal scales for the investigation of subsurface flow processes. *Hydrology and Earth System Sciences* **13** (7): 1215–1233 DOI: 10.5194/hess-13-1215-2009

Bogena HR, Bol R, Borchard N, Brüggemann N, Diekkrüger B, Drüe C, Groh J, Gottselig N, Huisman JA, Lücke A, et al. 2015. A terrestrial observatory approach to the integrated investigation of the effects of deforestation on water, energy, and matter fluxes. SCIENCE CHINA Earth Sciences **58** (1): 61–75 DOI: 10.1007/s11430-014-4911-7

Bogena H. 2021. TERENO (Eifel-Rur), SoilNet Wuestebach Available at: https://ddp.tereno.net/ddp/dispatch?searchparams=freetext-soilnet&metadata.detail.view.id=d4b917ca-4e8b-3b0f-8f24-5475f7390d99&metadata.detail.view.origin=EIFEL.RUR&metadata.detail.view.type=org.fzj.ibg.catalog.shared.ISO19115Bean [Accessed April 1, 2021]

Bongiovanni T, Caldwell TG. 2019. Texas Soil Observation Network (Texas) DOI: 10.18738/T8/JJ16CF

Boorman DB, Hollis JM, Lilly A. 1995. *Hydrology of soil types: a hydrologically-based classification of the soils of United Kingdom*. Institute of Hydrology. Available at: http://nora.nerc.ac.uk/id/eprint/7369/1/IH_126.pdf [Accessed April 1, 2021]

Bormann H, Klaassen K. 2008. Seasonal and land use dependent variability of soil hydraulic and soil hydrological properties of two Northern German soils. *Geoderma* **145** (3): 295–302 DOI: 10.1016/j.geoderma.2008.03.017

Bouaziz LJE, Fenicia F, Thirel G, de Boer-Euser T, Buitink J, Brauer CC, De Niel J, Dewals BJ, Drogue G, Grelier B, et al. 2021. Behind the scenes of streamflow model performance. *Hydrology and Earth System Sciences* **25** (2): 1069–1095 DOI: 10.5194/hess-25-1069-2021

Branger F, McMillan HK. 2020. Deriving hydrological signatures from soil moisture data. *Hydrological processes* **34** (6): 1410–1427 DOI: 10.1002/hyp.13645

Brocca L, Morbidelli R, Melone F, Moramarco T. 2007. Soil moisture spatial variability in experimental areas of central Italy. *Journal of Hydrology* **333** (2): 356–373 DOI: 10.1016/j.jhydrol.2006.09.004

Bureau of Economic Geology. 2020. Texas Soil Observation Network (Texas) Available at: https://www.beg.utexas.edu/research/programs/Texas [Accessed April 1, 2021]

Caldwell TG, Bongiovanni T, Cosh MH, Jackson TJ, Colliander A, Abolt CJ, Casteel R, Larson T, Scanlon BR, Young MH. 2019. The Texas Soil Observation Network:A Comprehensive Soil Moisture Dataset for Remote Sensing and Land Surface Model Validation. *Vadose zone journal: VZJ* **18** (1): 1–20 DOI: 10.2136/vzj2019.04.0034

Chandler DG, Seyfried MS, McNamara JP, Hwang K. 2017. Inference of soil hydrologic parameters from electronic soil moisture records. *Frontiers of Earth Science in China* **5** (April): 1–17 DOI: 10.3389/feart.2017.00025

Chen X, Liu L, Bartsch A. 2019. Detecting soil freeze/thaw onsets in Alaska using SMAP and ASCAT data. *Remote sensing of environment* **220**: 59–70 DOI: 10.1016/j.rse.2018.10.010

De Lannoy GJM, Verhoest NEC, Houser PR, Gish TJ, Van Meirvenne M. 2006. Spatial and temporal characteristics of soil moisture in an intensively monitored agricultural field (OPE3). *Journal of Hydrology* **331** (3–4): 719–730 DOI: 10.1016/j.jhydrol.2006.06.016

Detty JM, McGuire KJ. 2010. Threshold changes in storm runoff generation at a till-mantled headwater catchment. *Water resources research* **46** (7) DOI: 10.1029/2009wr008102

Deng L, Yan W, Zhang Y, Shangguan Z. 2016. Severe depletion of soil moisture following land-use changes for ecological restoration: Evidence from northern China. *Forest ecology and management* **366**: 1–10 DOI: 10.1016/j.foreco.2016.01.026

Dente L, Vekerdy Z, Wen J, Su Z. 2012. Maqu network for validation of satellite-derived soil moisture products. *International Journal of Applied Earth Observation and Geoinformation* **17** (1): 55–65 DOI: 10.1016/j.jag.2011.11.004

D'Odorico P, Ridolfi L, Porporato A, Rodriguez-Iturbe I. 2000. Preferential states of seasonal soil moisture: The impact of climate fluctuations. *Water resources research* **36** (8): 2209–2219 DOI: 10.1029/2000WR900103

Dorigo WA, Wagner W, Hohensinn R, Hahn S, Paulik C, Xaver A, Gruber A, Drusch M, Mecklenburg S, van Oevelen P, et al. 2011. The International Soil Moisture Network: a data hosting facility for global in situ soil moisture measurements. *Hydrology and Earth System Sciences* **15** (5): 1675–1698 DOI: 10.5194/hess-15-1675-2011

Dorigo WAA, Xaver A, Vreugdenhil M, Gruber A, Hegyiová A, Sanchis-Dufau ADD, Zamojski D, Cordes C, Wagner W, Drusch M. 2013. Global Automated Quality Control of In Situ Soil Moisture Data from the International Soil Moisture Network. *Vadose Zone Journal* **12** (3): vzj2012.0097-vzj2012.0097

Draper C, Reichle R. 2015. The impact of near-surface soil moisture assimilation at subseasonal, seasonal, and inter-annual timescales. *Hydrology and Earth System Sciences* **19** (12): 4831–4844 DOI: 10.5194/hess-19-4831-2015

Eltahir EAB. 1998. A Soil Moisture-Rainfall Feedback Mechanism: 1. Theory and observations. *Water resources research* **34** (4): 765–776 DOI: 10.1029/97WR03499

Entekhabi D, Narendra Das, Njoku E, Yueh S, Johnson J, Shi J. 2014. Soil Moisture Active Passive (SMAP) Algorithm Theoretical Basis Document Level 2 & 3 Soil Moisture (Passive) Data Products. Revision A. California, United States. Available at: https://nsidc.org/sites/nsidc.org/files/technical-references/L2_SM_P_ATBD_revision_C_Dec2016_v2.pdf [Accessed April 1, 2021]

Friedl MA, Sulla-Menashe D, Tan B, Schneider A, Ramankutty N, Sibley A, Huang X. 2010. MODIS Collection 5 global land cover: Algorithm refinements and characterization of new datasets. *Remote sensing of environment* **114** (1): 168–182 DOI: 10.1016/j.rse.2009.08.016

Fu B, Wang J, Chen L, Qiu Y. 2003. The effects of land-use on soil moisture variation in the Danangou catchment of the Loess Plateau, China. *Catena* **54** (1): 197–213 DOI: 10.1016/S0341-8162(03)00065-1

Gao X, Wu P, Zhao X, Wang J, Shi Y. 2014. Effects of land-use on soil moisture variations in a semi-arid catchment: implications for land and agricultural water management. *Land Degradation & Development* **25** (2): 163–172 DOI: 10.1002/ldr.1156

Ghannam K, Nakai T, Paschalis A, Oishi CA, Kotani A, Igarashi Y, Kumagai T, Katul GG. 2016. Persistence and memory timescales in root-zone soil moisture dynamics. *Water resources research* **52** (2): 1427–1445 DOI: 10.1002/2015WR017983

Gnann SJ, Coxon G, Woods RA, Howden NJK, McMillan HK. 2021a. TOSSH: A toolbox for streamflow signatures in hydrology. *Environmental Modelling and Software[R]* (104983): 104983 DOI: 10.1016/j.envsoft.2021.104983

Gnann SJ, McMillan HK, Woods RA, Howden NJK. 2021b. Including regional knowledge improves baseflow signature predictions in large sample hydrology. *Water resources research* **57** (2) DOI: 10.1029/2020wr028354

Graham CB, Lin HS. 2011. Controls and Frequency of Preferential Flow Occurrence: A 175-Event Analysis. *Vadose Zone Journal* **10** (3): 816–831 DOI: 10.2136/vzj2010.0119

Graham CB, Lin HS. 2012. The Hydropedograph Toolbox and its application. *Hydrology and Earth System Sciences Discussions* **9** (12): 14231–14271 DOI: 10.5194/hessd-9-14231-2012

Grayson RB, Western AW, Chiew FHS. 1997. Preferred states in spatial soil moisture patterns: *Water Resources Research* **33** (12): 2897–2908 DOI: 10.1029/97WR02174

Grayson RB, Western AW, Walker JP, Kandel DGD, Costelloe JF, Wilson DJ. 2006. Controls on patterns of soil moisture in arid and semi-arid systems., D'Odorico P, Porporato A (eds). Kluwer Academic Publishers: Netherland; 109–127.

Gómez-Plaza A, Martínez-Mena M, Albaladejo J, Castillo VM. 2001. Factors regulating spatial distribution of soil water content in small semiarid catchments. *Journal of Hydrology* **253** (1): 211–226 DOI: 10.1016/S0022-1694(01)00483-8

Gupta HV, Wagener T, Liu Y. 2008. Reconciling theory with observations: elements of a diagnostic approach to model evaluation. *Hydrological processes* **22** (18): 3802–3813 DOI: 10.1002/hyp.6989

Heudorfer B, Haaf E, Stahl K, Barthel R. 2019. Index-Based Characterization and Quantification of Groundwater Dynamics. *Water resources research* **55** (7): 5575–5592 DOI: 10.1029/2018WR024418

Horner I, Branger F, McMillan H, Vannier O, Braud I. 2020. Information content of snow hydrological signatures based on streamflow, precipitation and air temperature. *Hydrological processes* **34** (12): 2763–2779 DOI: 10.1002/hyp.13762

Hudson BD. 1994. Soil organic matter and available water capacity. *Journal of Soil and Water Conservation* **49** (2): 189

Jawson SD, Niemann JD. 2007. Spatial patterns from EOF analysis of soil moisture at a large scale and their dependence on soil, land-use, and topographic properties. *Advances in water resources* **30** (3): 366–381 DOI: 10.1016/j.advwatres.2006.05.006

Korres W, Reichenau TGG, Fiener P, Koyama CNN, Bogena HRR, Cornelissen T, Baatz R, Herbst M, Diekkrüger B, Vereecken H, et al. 2015. Spatio-temporal soil moisture patterns - A meta-analysis using plot to catchment scale data. *Journal of Hydrology* **520**: 326–341 DOI: 10.1016/j.jhydrol.2014.11.042

Koster RD, Suarez MJ. 2001. Soil moisture memory in climate models. *Journal of Hydrometeorology* **2** (6): 558–570 DOI: 10.1175/1525-7541(2001)002<0558:SMMICM>2.0.CO;2

Kruskal WH, Wallis WA. 1952. Use of Ranks in One-Criterion Variance Analysis. *Journal of the American Statistical Association* **47** (260): 583–621 DOI: 10.1080/01621459.1952.10483441

Kumar S, Newman M, Wang Y, Livneh B. 2019. Potential Reemergence of Seasonal Soil Moisture Anomalies in North America. *Journal of climate* **32** (10): 2707–2734 DOI: 10.1175/JCLI-D-18-0540.1

Laio F. 2002. On the seasonal dynamics of mean soil moisture. *Journal of geophysical research* **107** (D15) DOI: 10.1029/2001jd001252

Laio F, Porporato A, Fernandez-Illescas CP, Rodriguez-Iturbe I. 2001. Plants in water-controlled ecosystems: Active role in hydrologic processes and responce to water stress IV. Discussion of real cases. *Advances in water resources* **24** (7): 745–762 DOI: 10.1016/S0309-1708(01)00007-0

Lawston PM, Santanello JA Jr, Kumar SV. 2017. Irrigation Signals Detected From SMAP Soil Moisture Retrievals. *Geophysical research letters* **44** (23): 11,860–11,867 DOI: 10.1002/2017GL075733

Liang W-L, Kosugi K, Mizuyama T. 2011. Soil water dynamics around a tree on a hillslope with or without rainwater supplied by stemflow: SOIL WATER DYNAMICS WITH OR WITHOUT STEMFLOW. *Water resources research* **47** (2) DOI: 10.1029/2010wr009856

Mälicke M, Hassler SK, Blume T, Weiler M, Zehe E. 2020. Soil moisture: variable in space but redundant in time. *Hydrology and Earth System Sciences* **24** (5): 2633–2653 DOI: 10.5194/hess-24-2633-2020

Martini E, Wollschläger U, Kögler S, Behrens T, Dietrich P, Reinstorf F, Schmidt K, Weiler M, Werban U, Zacharias S. 2015. Spatial and Temporal Dynamics of Hillslope-Scale Soil Moisture Patterns: Characteristic States and Transition Mechanisms. *Vadose Zone Journal* **14** (4): vzj2014.10.0150-vzj2014.10.0150 10.2136/vzj2014.10.0150

McColl KA, He Q, Lu H, Entekhabi D. 2019. Short-term and long-term surface soil moisture memory time scales are spatially anticorrelated at global scales. *Journal of hydrometeorology* **20** (6): 1165–1182 10.1175/jhm-d-18-0141.1

McDonnell JJ, Sivapalan M, Vaché K, Dunn S, Grant G, Haggerty R, Hinz C, Hooper R, Kirchner J, Roderick ML, et al. 2007. Moving beyond heterogeneity and process complexity: A new vision for watershed hydrology. *Water resources research* **43** (7): 1–6 DOI: 10.1029/2006WR005467

McKnight DM. 2017. Debates-Hypothesis testing in hydrology: A view from the field: The value of hydrologic hypotheses in designing field studies and interpreting the results to advance hydrology: HYPOTHESES OF ONE KIND OR ANOTHER. *Water resources research* **53** (3): 1779–1783 DOI: 10.1002/2016WR020050

McMillan H. 2020. Linking hydrologic signatures to hydrologic processes: A review. *Hydrological processes* **34** (6): 1393–1409 DOI: 10.1002/hyp.13632

McMillan H. 2020b. A review of hydrologic signatures and their applications. *WIREs Water* **8** (1): DOI: 10.1002/wat2.1499

McMillan H, Srinivasan MS. 2015. Characteristics and controls of variability in soil moisture and groundwater in a headwater catchment. *Hydrology and Earth System Sciences* **19** (4): 1767–1786 DOI: 10.5194/hess-19-1767-2015

869 McMillan H, Gueguen M, Grimon E, Woods R, Clark M, Rupp DE. 2014. Spatial variability of hydrological processes and model structure diagnostics in a 50 km 2 catchment. *Hydrological processes* **28** (18): 4896–4913 DOI: 10.1002/hyp.9988

872 McMillan H, Westerberg I, Branger F. 2017. Five guidelines for selecting hydrological signatures. *Hydrological processes* **31** (26): 4757–4761 DOI: 10.1002/hyp.11300

874 Miguez-Macho G, Fan Y. 2012. The role of groundwater in the Amazon water cycle: 2. Influence on seasonal soil moisture and evapotranspiration. *Journal of geophysical research* **117** (D15) DOI: 10.1029/2012jd017540

877 Morel, 2018. Gramm: grammar of graphics plotting in Matlab. *Journal of Open Source Software* **3** (23), 568 DOI:10.21105/joss.00568

879 National Aeronautics and Space Administration (NASA), National Imagery and Mapping Agency (NIMA), German Aerospace Center (DLR), Italian Space Agency (ASI). 2002. Shuttle Radar Topography Mission (SRTM) Elevation Dataset Available at: http://seamless.usgs.gov [Accessed May 8, 2021]

883 Penna D, Tromp-Van Meerveld HJ, Gobbi A, Borga M, Dalla Fontana G. 2011. The influence of soil moisture on threshold runoff generation processes in an alpine headwater catchment. *Hydrology and Earth System Sciences* **15** (3): 689–702 DOI: 10.5194/hess-15-689-2011

887 Potter NJ, Zhang L, Milly PCD, McMahon TA, Jakeman AJ. 2005. Effects of rainfall seasonality and soil moisture capacity on mean annual water balance for Australian catchments: WATER BALANCE OF AUSTRALIAN CATCHMENTS. *Water resources research* **41** (6) DOI: 10.1029/2004wr003697

891 Richter BD, Baumgartner JV, Braun JP, B DPB. 1996. A Method for Assessing Hydrologic Alteration within Ecosystems. *Conservation biology: the journal of the Society for Conservation Biology* **10** (Aug): 1163–1174 DOI: 10.1007/s13361-012-0389-8

894 Riffenburgh RH. 2006. Chapter Summaries. In *Statistics in Medicine*, Riffenburgh RH (ed.). Elsevier: San Diego, CA; 533–580. DOI: 10.1016/b978-012088770-5/50067-8

896 Rodriguez-Iturbe I, D'Odorico P, Porporato A, Ridolfi L. 1999a. On the spatial and temporal links between vegetation, climate, and soil moisture. *Water resources research* **35** (12): 3709–3722 DOI: 10.1029/1999wr900255

899 Rodriguez-Iturbe I, Porporato A, Ridolfi L, Isham V, Coxi DR. 1999b. Probabilistic modelling of water balance at a point: the role of climate, soil and vegetation.

Proceedings of the Royal Society of London. Series A: Mathematical, Physical and Engineering Sciences **455** (1990): 3789–3805 DOI: 10.1098/rspa.1999.0477

Rogger M, Agnoletti M, Alaoui A, Bathurst JC, Bodner G, Borga M, Chaplot V, Gallart F, Glatzel G, Hall J, et al. 2017. Land-use change impacts on floods at the catchment scale: Challenges and opportunities for future research. *Water resources research* **53** (7): 5209–5219 DOI: 10.1002/2017WR020723

Rosenbaum U, Bogena HR, Herbst M, Huisman JA, Peterson TJ, Weuthen A, Western AW, Vereecken H. 2012. Seasonal and event dynamics of spatial soil moisture patterns at the small catchment scale. *Water resources research* **48** (10): 1–22 DOI: 10.1029/2011WR011518

Selassie YG, Ayanna G. 2013. Effects of different land use systems on selected physico-chemical properties of soils in Northwestern Ethiopia. *Journal of Agricultural Science* **5** (4): 112 DOI: 10.5539/jas.v5n4p112

Samuel JM, Sivapalan M, Struthers I. 2008. Diagnostic analysis of water balance variability: A comparative modeling study of catchments in Perth, Newcastle, and Darwin, Australia. *Water resources research* **44** (6): 1–13 DOI: 10.1029/2007WR006694

Sawicz K, Wagener T, Sivapalan M, Troch PA, Carrillo G. 2011. Catchment classification: empirical analysis of hydrologic similarity based on catchment function in the eastern USA. *Hydrology and Earth System Sciences Discussions* **8** (3): 4495–4534 DOI: 10.5194/hessd-8-4495-2011

Schaefli B. 2016. Snow hydrology signatures for model identification within a limits-of-acceptability approach. *Hydrological processes* **30** (22): 4019–4035 DOI: 10.1002/hyp.10972

Shafii M, Tolson BA. 2015. Optimizing hydrological consistency by incorporating hydrological signatures into model calibration objectives. *Water resources research* **51** (5): 3796–3814 DOI: 10.1002/2014wr016520

Singh VP, Frevert DK. 2010. *Watershed Models*. CRC Press.

Skøien JO, Blöschl G, Western AW. 2003. Characteristic space scales and timescales in hydrology: CHARACTERISTIC SCALES IN HYDROLOGY. *Water resources research* **39** (10) DOI: 10.1029/2002wr001736

Smith AB, Walker JP, Western AW, Young RI, Ellett KM, Pipunic RC, Grayson RB, Siriwardena L, Chiew FHS, Richter H. 2012. The Murrumbidgee soil moisture monitoring network data set. *Water resources research* 48 (7) DOI: 10.1029/2012WR011976

Soylu ME, Bras RL. 2021. Detecting shallow groundwater from spaceborne soil moisture observations. *Water resources research* **57** (2) DOI: 10.1029/2020wr029102

Su Z, Wen J, Dente L, van der Velde R, Wang L, Ma Y, Yang K, Hu Z. 2011. The Tibetan Plateau observatory of plateau scale soil moisture and soil temperature (Tibet-Obs) for quantifying uncertainties in coarse resolution satellite and model products. *Hydrology and Earth System Sciences* **15** (7): 2303–2316 DOI: 10.5194/hess-15-2303-2011

Sumargo E, McMillan H, Weihs R, Ellis CJ, Wilson AM, Ralph FM. 2021. A Soil Moisture Monitoring Network to Assess Controls on Runoff Generation During Atmospheric River Events. *Hydrological processes* **35** (1) DOI: 10.1002/hyp.13998

Teuling AJ, Uijlenhoet R, Troch PA. 2005. On bimodality in warm season soil moisture observations. *Geophysical research letters* **32** (June): 10–13 DOI: 10.1029/2005GL023223

The Deutscher Wetterdienst (DWD). 2021. Open Data Server, climate data provided by DWD's Climate Data Center Available at: https://opendata.dwd.de/climate_environment/CDC/ [Accessed April 1, 2021]

The Royal Netherlands Meteorological Institute (KNMI). 2021. Dagwaarden neerslagstations (Daily values of precipitation stations) Available at: https://www.knmi.nl/nederland-nu/klimatologie/monv/reeksen [Accessed April 1, 2021]

Tian J, Zhang B, He C, Han Z, Bogena HR, Huisman JA. 2019. Dynamic response patterns of profile soil moisture wetting events under different land covers in the Mountainous area of the Heihe River Watershed, Northwest China. *Agricultural and Forest Meteorology* **271**: 225–239 DOI: 10.1016/j.agrformet.2019.03.006

Trimble SW. 2007. *Encyclopedia of water Science*. CRC Press.

Tromp-van Meerveld HJ, McDonnell JJ. 2006. On the interrelations between topography, soil depth, soil moisture, transpiration rates and species distribution at the hillslope scale. *Advances in water resources* **29** (2): 293–310 DOI: 10.1016/j.advwatres.2005.02.016

University of Hamburg. 2021. HUSCO-Hamburg Urban Soil Climate Observatory (2010-2016, project completed). *CliSAP* Available at: https://www.clisap.de/research/b:-

climate-manifestations-and-impacts/b5:-urban-systems-test-bed-hamburg/husco-hamburg-urban-soil-climate-observatory/ [Accessed April 1, 2021]

Vanderlinden K, Vereecken H, Hardelauf H, Herbst M, Martínez G, Cosh MH, Pachepsky YA. 2012. Temporal Stability of Soil Water Contents: A Review of Data and Analyses. *Vadose Zone Journal* **11** (4): vzj2011.0178-vzj2011.0178 DOI: 10.2136/vzj2011.0178

Vereecken H, Kamai T, Harter T, Kasteel R, Hopmans J, Vanderborght J. 2007. Explaining soil moisture variability as a function of mean soil moisture: A stochastic unsaturated flow perspective. *Geophysical research letters* **34** (22) DOI: 10.1029/2007gl031813

Vereecken H, Schnepf A, Hopmans JWW, Javaux M, Or D, Roose T, Vanderborght J, Young MHH, Amelung W, Aitkenhead M, et al. 2016. Modeling soil processes: Review, key challenges, and new perspectives. *Vadose Zone Journal* **15** (5): vzj2015.09.0131-vzj2015.09.0131 DOI: http://dx.doi.org/10.2136/vzj2015.09.0131

Viglione A, Merz B, Viet Dung N, Parajka J, Nester T, Blöschl G. 2016. Attribution of regional flood changes based on scaling fingerprints. *Water resources research* **52** (7): 5322–5340 DOI: 10.1002/2016WR019036

Wagener T, Sivapalan M, Troch P, Woods R. 2007. Catchment classification and hydrologic similarity. *Geography compass* **1** (4): 901–931 DOI: 10.1111/j.1749-8198.2007.00039.x

Wang J, Luo S, Li Z, Wang S, Li Z. 2019. The freeze/thaw process and the surface energy budget of the seasonally frozen ground in the source region of the Yellow River. *Theoretical and Applied Climatology* **138** (3–4): 1631–1646 DOI: 10.1007/s00704-019-02917-6

Western AW, Zhou S-LL, Grayson RB, Wilson DJ, Mcmahon TA, Blöschl G, Wilson DJ. 2004. Spatial correlation of soil moisture in small catchments and its relationship to dominant spatial hydrological processes. *Journal of Hydrology* **286** (1-4): 113–134 DOI: 10.1016/j.jhydrol.2003.09.014

Wiekenkamp I, Huisman JA, Bogena HR, Lin HS, Vereecken H. 2016a. Spatial and temporal occurrence of preferential flow in a forested headwater catchment. *Journal of Hydrology* **534**: 139–149 DOI: 10.1016/j.jhydrol.2015.12.050

Wiekenkamp I, Huisman JA, Bogena HR, Graf A, Lin HS, Drüe C, Vereecken H. 2016b. Changes in measured spatiotemporal patterns of hydrological response after partial deforestation in a headwater catchment. Journal of Hydrology **542**: 648–661 DOI: 10.1016/J.JHYDROL.2016.09.037

Wiekenkamp I, Huisman JA, Bogena HR, Vereecken H. 2019. Effects of Deforestation on Water Flow in the Vadose Zone. *WATER* **12** (1): 35–35 DOI: 10.3390/w12010035

Wiesner S, Eschenbach A, Ament F. 2014. Urban air temperature anomalies and their relation to soil moisture observed in the city of Hamburg. *Meteorologische Zeitschrift* **23** (2): 143–157 DOI: 10.1127/0941-2948/2014/0571

Wiesner S, Gröngröft A, Ament F, Eschenbach A. 2016. Spatial and temporal variability of urban soil water dynamics observed by a soil monitoring network. *Journal of soils and sediments* **16** (11): 2523–2537 DOI: 10.1007/s11368-016-1385-6

Westerberg IK, Guerrero J-L, Younger PM, Beven KJ, Seibert J, Halldin S, Freer JE, Xu C-Y. 2011. Calibration of hydrological models using flow-duration curves. Hydrology and Earth System Sciences **15** (7): 2205–2227 DOI: 10.5194/hess-15-2205-2011

Woodruff CM, Wilding LP. 2008. Bedrock, soils, and hillslope hydrology in the Central Texas Hill Country, USA: Implications on environmental management in a carbonate-rock terrain. *Environmental geology* **55** (3): 605–618 DOI: 10.1007/s00254-007-1011-4

Yarnell SM, Petts GE, Schmidt JC, Whipple AA, Beller EE, Dahm CN, Goodwin P, Viers JH. 2015. Functional Flows in Modified Riverscapes: Hydrographs, Habitats and Opportunities. *Bioscience* **65** (10): 963–972 DOI: 10.1093/biosci/biv102

Young R, Walker JP, Yeoh N, Smith A, Ellett K, Merlin O, Western AW. 2008. Soil moisture and meteorological observations from the Murrumbidgee catchment. Available at: http://www.Oznet.org.au/documentation/Soil_Moisture_Meteorological_Observation_of_Murrumbidgee_Catchment.pdf

Zehe E, Becker R, Bárdossy A, Plate E. 2005. Uncertainty of simulated catchment runoff response in the presence of threshold processes: Role of initial soil moisture and precipitation. *Journal of Hydrology* **315** (1–4): 183–202 DOI: 10.1016/j.jhydrol.2005.03.038

Ziegler AD, Giambelluca TW, Sutherland RA, Vana TT, Nullet MA. 2001. Horton overland flow contribution to runoff on unpaved mountain roads: A case study in northern Thailand. *Hydrological processes* **15** (16): 3203–3208 DOI: 10.1002/hyp.480

1028 **SUPPORTING INFORMATION**

1029 The supplementary material includes the following.

1030 **Text S1** describes quality control procedures of soil moisture data

1031 **Table S1** describes sensor configurations of the study site

1032 **Figure S1** shows the results of the statistical test for signature profiles with soil depths

1033 between land-uses

1034 **Figure S2, 3, 4** shows all the results for event-based, season-based, and timeseries-based

1035 signatures, respectively

1036 **Text S2 and Figure S5** describe the applicability of signatures for diverse types of time

1037 series of data

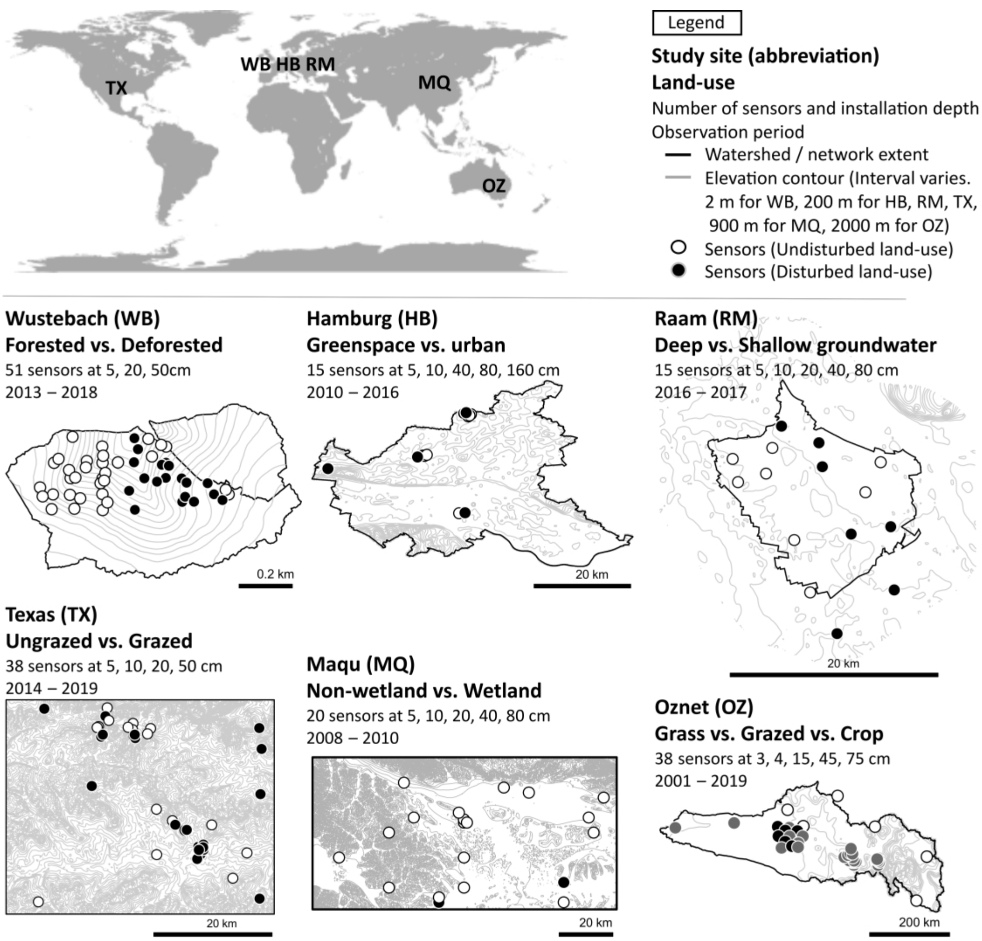

FIGURE 1 Maps of the study sites. The contours are based on a field survey for WB (Graf et al., 2014), Shuttle Radar Topography Mission Elevation Dataset (National Aeronautics and Space Administration (NASA) et al., 2002) for HB, RM, TX, MQ, and OZ. All maps are north upward

481x451mm (236 x 236 DPI)

(a)

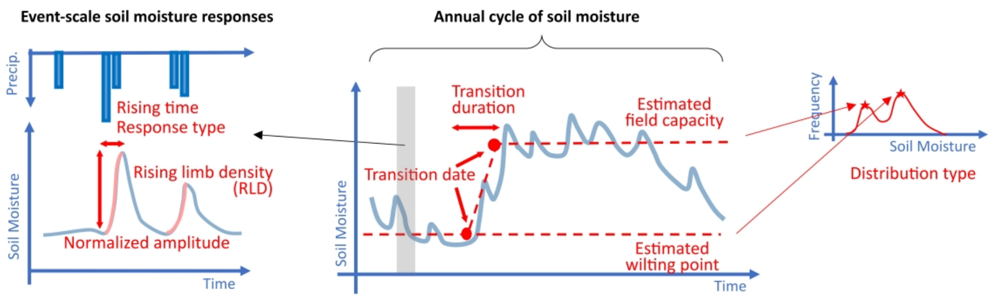

(b)

		Timescale		
		Event	**Season**	**Complete timeseries**
Dynamics	**Shape**	Rising limb density (Sawicz *et al*., 2011)	-	Distribution type (Branger & McMillan, 2019; Graham and Lin, 2012)
	Timing	Response type (Graham and Lin, 2012; Wiekenkamp *et al*., 2016)	Transition date (Branger & McMillan, 2019)	-
	Speed	Rising time (Branger & McMillan 2019)	Transition duration (Branger & McMillan, 2019)	-
	Magnitude	Normalized amplitude (Branger & McMillan, 2019)	-	Estimated field capacity Estimated wilting point (Branger & McMillan, 2019; Chandler *et al*., 2017)

FIGURE 2 A set of signatures describing the soil moisture dynamics. (a) Illustrations show the signatures calculated. (b) A table shows the aspects of soil moisture dynamics represented by the signatures

582x464mm (236 x 236 DPI)

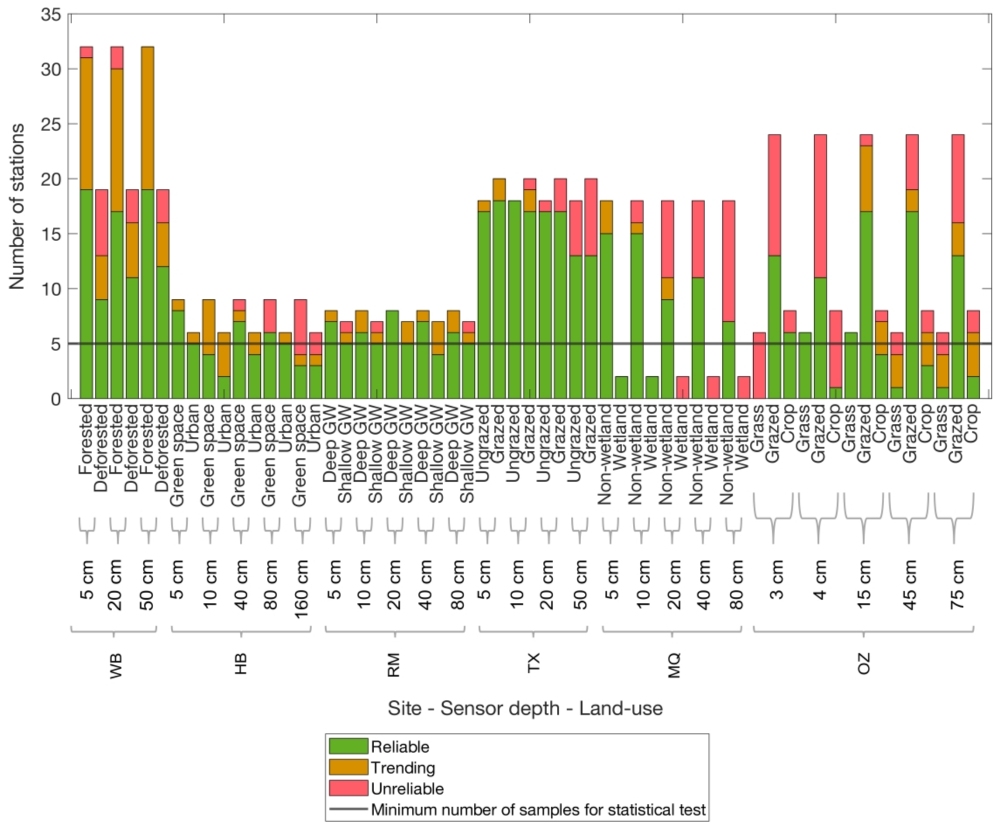

FIGURE 3 Number of stations that passed the final quality control. The categories that have five or more variables can be used for statistical analysis (indicated by a horizontal line)

694x577mm (236 x 236 DPI)

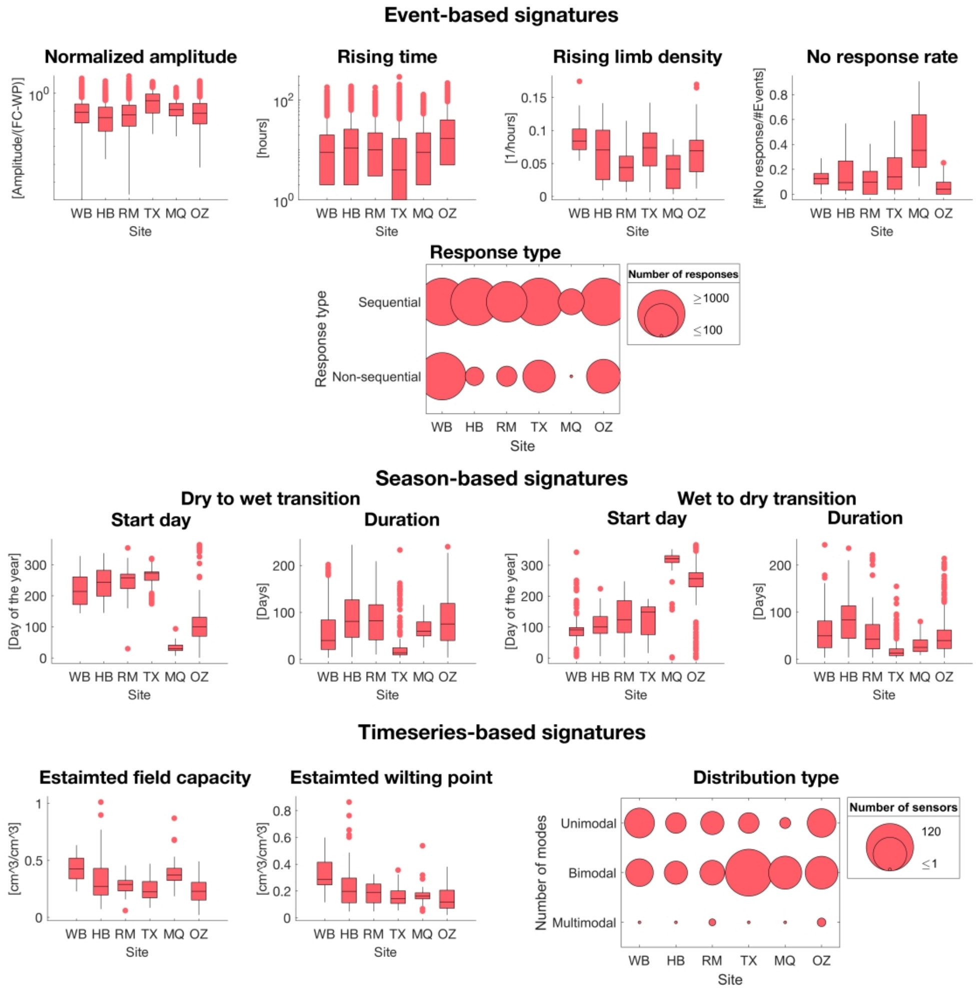

FIGURE 4 Signature values for all the study sites, in the order of aridity (large to small from left to right based on the aridity values listed in Table 1). Signature values were aggregated for sensor depths and land-uses. The boxplots are drawn using Matlab package gramm (Morel, 2018). The box is drawn between the first and third quartile, with a line in between indicating the median. The whiskers extended within a distance to the box equal to 1.5 times the interquartile range. Dots indicate the outliers

543x561mm (236 x 236 DPI)

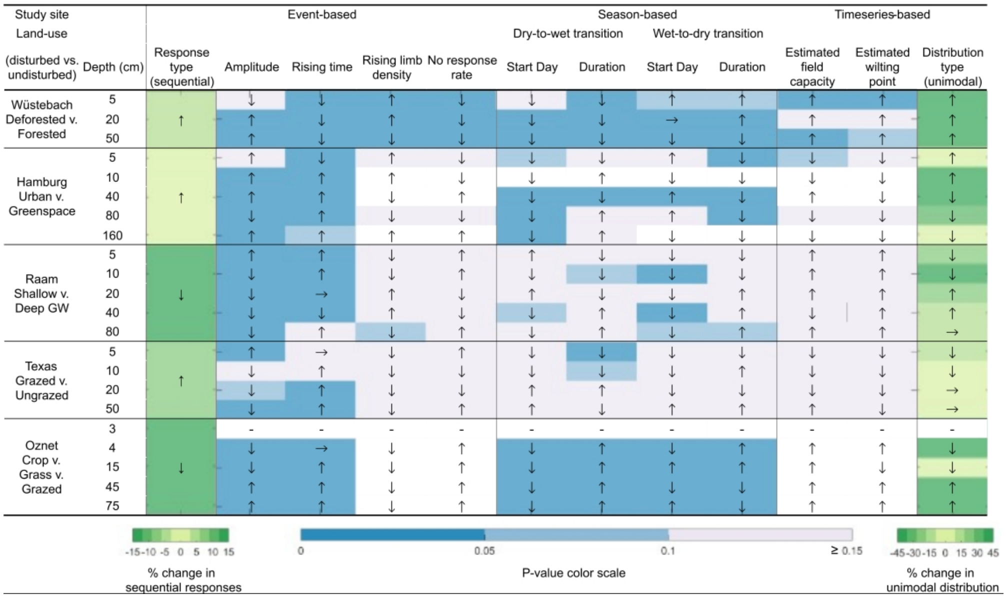

Study site / Land-use (disturbed vs. undisturbed)	Depth (cm)	Event-based: Response type (sequential)	Event-based: Amplitude	Event-based: Rising time	Event-based: Rising limb density	Event-based: No response rate	Season-based, Dry-to-wet transition: Start Day	Season-based, Dry-to-wet transition: Duration	Season-based, Wet-to-dry transition: Start Day	Season-based, Wet-to-dry transition: Duration	Timeseries-based: Estimated field capacity	Timeseries-based: Estimated wilting point	Timeseries-based: Distribution type (unimodal)
Wüstebach Deforested v. Forested	5	↑	↓	↓	↑	↓	↓	↓	↑	↑	↑	↑	↑
	20		↑	↓	↑	↓	↓	↓	→	↑	↑	↑	↑
	50		↑	↓	↓	↓	↓	↓	↓	↓	↑	↑	↑
Hamburg Urban v. Greenspace	5	↑	↑	↓	↑	↓	↓	↓	↑	↓	↓	↓	↑
	10		↑	↑	↑	↓	↓	↑	↓	↓	↓	↓	↑
	40		↑	↑	↓	↑	↓	↓	↑	↓	↑	↓	↓
	80		↓	↑	↓	↓	↓	↑	↑	↓	↓	↓	↓
	160		↑	↑	↑	↑	↓	↑	↓	↓	↓	↓	↓
Raam Shallow v. Deep GW	5	↓	↑	↑	↓	↑	↑	↓	↓	↓	↑	↑	↓
	10		↓	↑	↓	↑	↓	↓	↓	↓	↑	↑	↓
	20		↓	→	↑	↓	↑	↓	↓	↑	↑	↑	↑
	40		↓	↓	↑	↓	↓	↑	↓	↑	↓	↑	↑
	80		↓	↑	↓	↑	↓	↑	↓	↑	↑	↑	→
Texas Grazed v. Ungrazed	5	↑	↑	→	↓	↑	↓	↓	↓	↓	↓	↓	↓
	10		↓	↑	↓	↓	↓	↓	↓	↑	↓	↓	↓
	20		↓	↑	↓	↓	↑	↑	↓	↓	↓	↓	→
	50		↓	↑	↓	↑	↑	↓	↑	↑	↑	↓	→
Oznet Crop v. Grass v. Grazed	3	↓	-	-	-	-	-	-	-	-	-	-	-
	4		↓	→	↓	↑	↓	↑	↓	↑	↑	↑	↓
	15		↓	↑	↓	↑	↓	↑	↑	↑	↑	↓	↓
	45		↑	↑	↓	↑	↓	↑	↓	↓	↑	↑	↑
	75		↑	↑	↓	↑	↓	↑	↑	↓	↑	↑	↑

FIGURE 5 Signature differences in magnitude between contrasting land-uses for a given depth. In each study site, signatures from a disturbed land-use were compared with those from an undisturbed land-use (e.g., deforested as disturbed vs. forested as undisturbed). The upward, downward, and horizontal arrows indicate if the signature values in the disturbed land-use were larger, smaller, or unchanged, respectively, compared to undisturbed land-use. The cells are highlighted with colors associated with the p-value of the Kruskal–Wallis test, or percent change in signature dominance. The cells are white when the sample size was not enough for the Kruskal-Wallis test (less than five). Most signatures for the Maqu sites did not reach enough sample size for the Kruska-Wallis test; thus, they were excluded from the table

601x355mm (236 x 236 DPI)

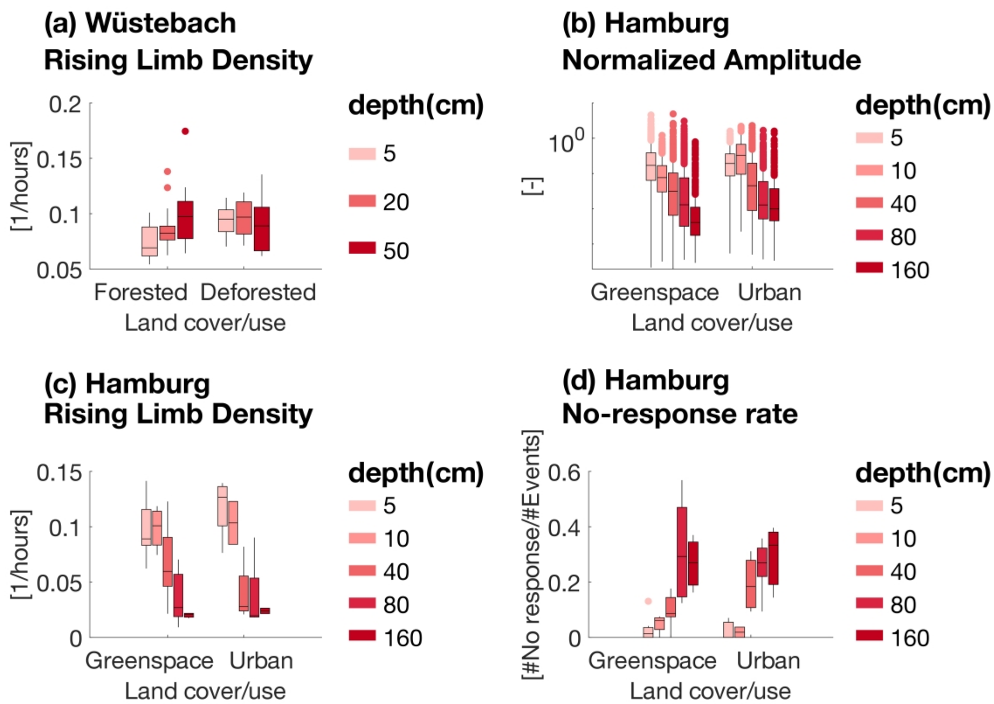

FIGURE 6 Box plots of event-based signatures for the sites showing significant differences in signatures. Refer to Figure S2 for full results. The box is drawn between the first and third quartile, with a line in between indicating the median. The whiskers extend to the most extreme data value within a distance to the box equal to 1.5 times the interquartile range. Dots indicate the outliers

757x539mm (236 x 236 DPI)

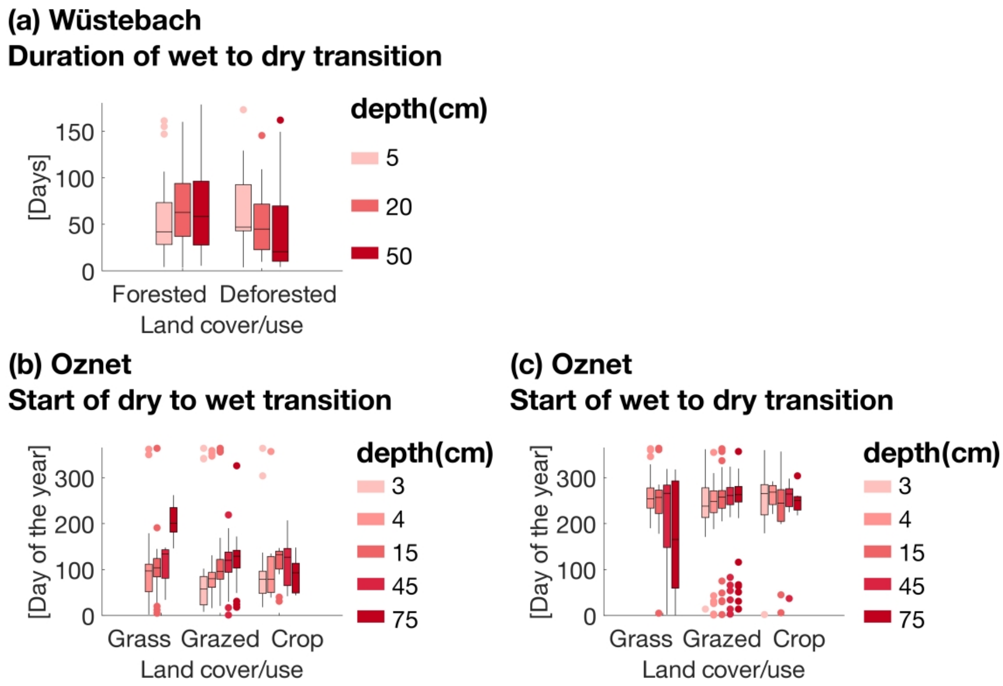

FIGURE 7 Box plots of season-based signatures for the sites showing significant differences in signatures. Refer to Figure S3 for full results. The box is drawn between the first and third quartile, with a line in between indicating the median. The whiskers extend to the most extreme data value within a distance to the box equal to 1.5 times the interquartile range. Dots indicate the outliers

750x519mm (236 x 236 DPI)

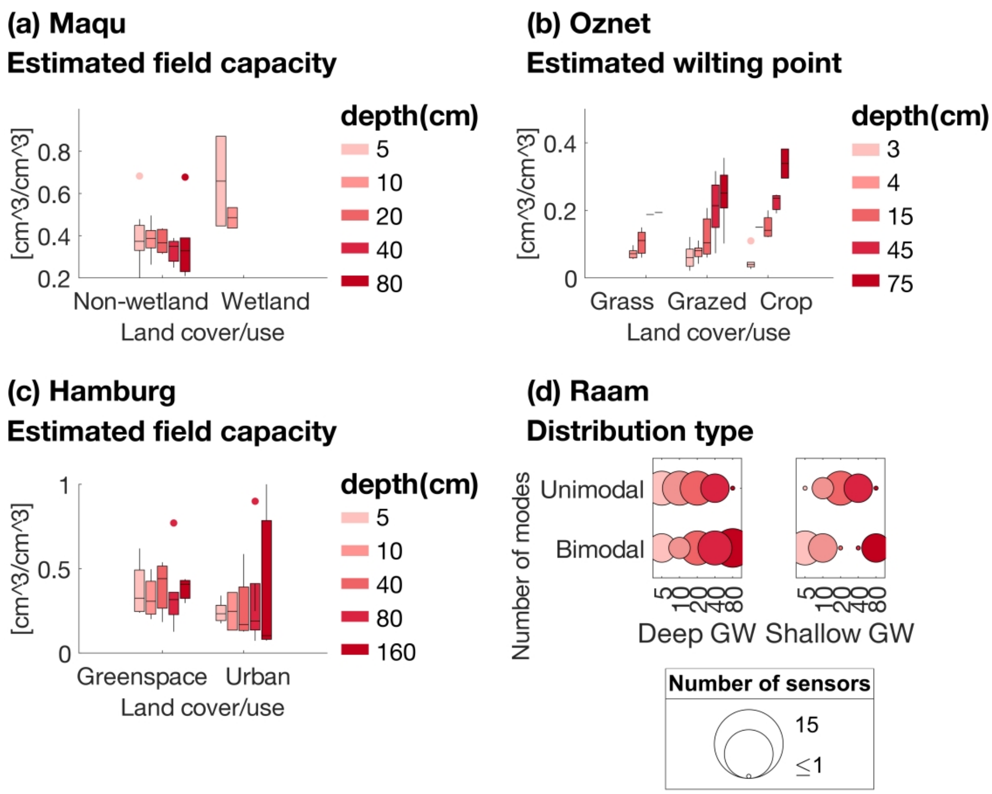

FIGURE 8 Box plots of timeseries-based signatures for the sites showing significant differences in signatures. Refer to Figure S4 for full results. The box is drawn between the first and third quartile, with a line in between indicating the median. The whiskers extend to the most extreme data value within a distance to the box equal to 1.5 times the interquartile range. Dots indicate the outliers

744x587mm (236 x 236 DPI)

		Signatures											
		Event-based					Season-based				Timeseries-based		
							Dry-to-wet transition		Wet-to-dry transition				
		Response type (% of sequential)	Amplitude	Rising time	Rising limb density	No-response rate	Start Day	Duration	Start Day	Duration	Field capacity	Wilting point	Distribution type (% of unimodal)
Wüstebach Deforested vs. Forested	Expected process	Sequential flow↑; no flow↓; storage flashiness↑ due to storage↑ (Wiekenkamp et al., 2016a & 2019)					Earlier transition due to interception↓ & rain rate↑ & root depth↓ (Wiekenkamp et al., 2016b; Laio, 2002); closer to transition threshold due to storage↑ (Detty & McGuire, 2010)				Storage↑ due to transpiration↓ & interception↓ (Wiekenkamp et al., 2016a)		
	Expected signature	↑	↑	↓	↑	↓	↓	↓	↓	↓	↑	↑	↑
	Observed signature	↑	↑	↓	shallow↑ deep↓	↓	↓	↓	→	shallow ↑ deep ↓	↑	↑	↑
Hamburg Housing vs. Urban	Expected process	Vertical infiltration -> overland flow due to surface sealing (Scalenghe & Ajmone-Marsan, 2009; Ziegler et al., 2001); storage flashiness↓ due to storage↓					Delayed transition due to surface sealing & rain rate↓ (Laio, 2002); stagnant water & rapid drainage due to construction waste (Wiesner et al., 2016); less close to transition threshold due to storage↓ (Detty & McGuire, 2010)				Storage↓& GW table↓ due to infiltration↓ (Scalenghe & Ajmone-Marsan, 2009; Wiesner et al., 2016)		
	Expected signature	↑	shallow↑ deep↓	shallow↓ deep↑	shallow↑ deep↓	shallow↓ deep↑	↑	↑	↑	↓ or ↑	↓ variability↑ in deep soil layer	↓	deep ↓
	Observed signature	↑	shallow↑ deep↑	shallow↓ deep↑	shallow↑ deep↓	shallow↓ deep↑	↓	→	→	↓	↓ variability↑ in deep soil layer	↓	shallow↑ deep↓
Raam Shallow vs. Deep groundwater (GW)	Expected process	Vertical infiltration -> lateral flow; less variable soil moisture due to near-saturated soil (Soylu & Bras, 2021)					Earlier transition due to shallow GW (Miguez-Macho & Fan, 2012); more close to transition threshold due to storage↑ (Detty & McGuire, 2010)				Storage↑ due to capillary rise (Benninga et al., 2018b; Soylu & Bras, 2020)		
	Expected signature	↓	↓	↓	→	→	↓	↓	↓	↓	↑	↑	↑
	Observed signature	↓	↓	↑	→	→	→	→	↓	→	→	→	shallow↓ deep↑
Texas Grazed vs. Ungrazed	Expected process	Vertical infiltration -> overland flow due to compaction (Woodruff & Wilding, 2008; Alaoui et al., 2018; Ziegler et al., 2001)					Less close to transition threshold due to storage↓ (Detty & McGuire, 2010)				Storage↓ due to compaction (Bormann & Klaassen, 2008; Selassie & Ayanna, 2013)		
	Expected signature	↑	shallow↑ deep↓	shallow↓ deep↑	shallow↑ deep↓	shallow↓ deep↑	→	↑	→	↑	↓	↓	↓
	Observed signature	↑	shallow↑ deep↓	↑	→	→	→	↓	→	→	→	→	→
Maqu Wetland vs. Non-wetland	Expected processes	Less variable soil moisture due to near-saturated soil (Soylu & Bras, 2021); less responses while frozen					Seasonal transition timing of vegetation growth do not change (Dente et al., 2012); Freeze/thaw process takes longer and delayed due to heat capacity↑				Storage↑ due to soil organic matter (Dente et al., 2012; Hudson et al., 2014)		
	Expected signature	↓	↓	↓	↓	↑	→ or ↑	→ or ↑	→ or ↑	→ or ↑	↑	↑	↑
	Observed signature	Not enough data	→	→	↓	↑	→	→	→	→	↑	↑	↑
Oznet Crop vs. Grazed vs. Grass	Expected process	Vertical infiltration -> overland-flow due to compaction (Alaoui et al., 2018; Ziegler et al., 2001); storage flashiness ↑ due to storage↑					More close to transition threshold due to storage↑(Detty & McGuire, 2010); extended wet period due to irrigation (Smith et al., 2012)				Storage↓ due to compaction (Bormann & Klaassen, 2008; Selassie & Ayanna, 2013); Storage↑ due to irrigation (Smith et al., 2012; Lawston et al., 2017)		
	Expected signature	↑	shallow↑ deep↓	shallow↓ deep↑	shallow↑ deep↓	shallow↓ deep↑	↓	↓	↑	↓	↓ or ↑	↓ or ↑	↓ or ↑
	Observed signature	↓	shallow↓ deep↑	↑	↓	↑	↓	↑	mixed ↑ & ↓	shallow ↑ deep ↓	↑	↑	shallow↓ deep↑

Observed signature matches with literature interpretation

Observed signature does not match with literature interpretation

FIGURE 9 Process-based interpretation of signature differences between land-uses in terms of signature magnitude. The cells are highlighted blue when the signature matched with literature values and red if not. 'Shallow' and 'deep' mean different behavior expected or observed depending on the soil depth

606x722mm (236 x 236 DPI)

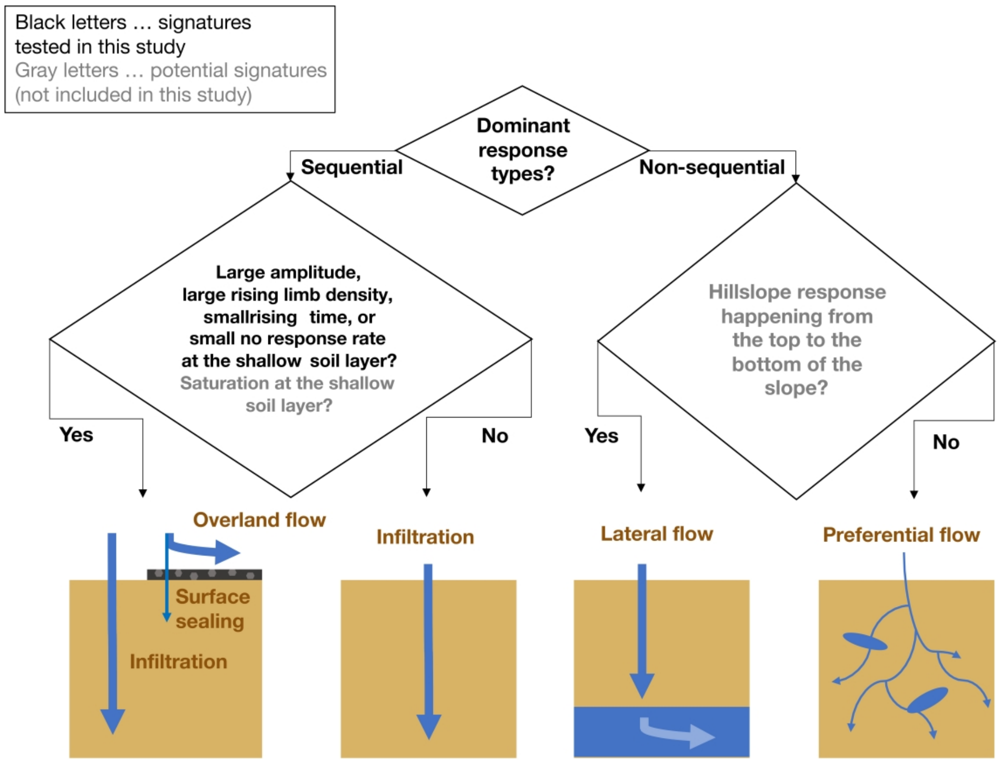

FIGURE 10 An example flow chart that classifies soil moisture dynamics using event-based soil moisture signatures

631x484mm (236 x 236 DPI)

TABLE 1 Key climatic and geological characteristics of study sites. The data are obtained from 'Key reference papers.' Aridity was calculated using GLDAS-2.1 (Rodell *et al.*, 2004) as the ratio of the annual total precipitation rate to the annual potential evaporation rate. For each station, aridity calculated at all sensor points and averaged for the observation period

Study site (abbreviation)	Land-use, in the order of degree of disturbance	Annual pre-cipitation (mm/yr)	Annual mean tempera-ture (°C)	Aridity	Vegetation	Soil type (texture and soil type)	Key reference papers
Wüstebach WB	Forested vs. deforested (Logging removed 97 % of tree biomass. Stumps and litter remained. Trees were transported by skid rails to minimize soil compaction)	1220	7 (< 0C Dec. to Mar.)	0.97	Coniferous trees (Norway Spruce and Sitka spruce) planted in the 1940s. Average density 370 trees/ha, average height 25 m	Silty clay loam with fractions of coarse material; Cambisols, Planosols, and Gleysols	(Rosenbaum *et al.*, 2012; Wiekenkamp *et al.*, 2019; Bogena *et al.*, 2015)
Hamburg HB	Greenspace vs. urban (The urban area mostly consists of housings. The degree of sealing is 50 – 60%. Soil moisture sensors were installed in the backyards. Soil profile contains construction waste)	775	Avg 9; max 17; min 1	0.78	Lawn, high pasture grass, short grass, and deciduous trees	Sand, sandy loam, loamy sand, and peat; Cambrisols, Technosol, Luvisol, Anthorosol, Greysol, Histosol, and Regosol	(Wiesner *et al.*, 2014, 2016)
Raam RM	Deep (>1m) vs. shallow groundwater (The definition follows Benninga et al., 2018). The groundwater table fluctuates 25 – 160 cm below the soil surface.)	818	Avg 9.1; max 18.3; min 3.3;	0.58	Grass	Sand with 20% loam content; Podzols and Anthorosols	(Benninga *et al.*, 2018b)
Texas TX	Ungrazed vs. grazed (The definition follows field note in the metadata)	807	18.4	0.40	Oak trees, woody plants (ashe juniper and honey mesquite), and grass	Sand, sandy loam, clay loam, silty clay, clay; Calciustolls, Haplustepts, Calciustepts	(Woodruff and Wilding, 2008; Caldwell *et al.*, 2019; Bureau of Economic Geology, 2020)
Maqu MQ	Non-wetland vs. wetland (Soil organic matter content is 17 – 56 g/kg and 136 – 229 g/kg, respectively)	593	1.3 (< 0C from Nov. to Mar.)	0.42	Grass	Silt loam; N/A	(Su *et al.*, 2011; Dente *et al.*, 2012; Wang *et al.*, 2019)
Oznet OZ	Grass vs. grazed vs. crop (The definition follows the metadata. Grazing is sheep, beef, and dairy. Cropping includes both irrigated- and non-irrigated method)	Varies (300 – 1900)	16	0.17	Grass, pasture, crops (rice, barley, and oats)	Silty loam; N/A	(Young *et al.*, 2008; Smith *et al.*, 2012)

SUPPLEMENTAL MATERIALS

TEXT S1 Data quality control

TEXT-S1.1. Quantitative control of short-term errors

We preprocessed soil moisture data for quality control. In most cases, data were preprocessed by each observatory based on its standards. We inspected the remaining errors automatically and manually as follows. First, errors were removed by quantitative assessment. Soil moisture value above 100%, sudden drops of more than 10% decrease in 1 hr, and sudden increases of more than 25% in 1 hr were removed automatically. Then, data gaps that were shorter than 3 hrs were filled by linear interpolation. Longer gaps were retained as no data. If there is a data fragment whose length is less than 5 days, the period of record was removed. Some stations (5 – 50% of stations, depending on the network) showed different mean soil moisture values during an initial settling-in period and/or later observation periods. To identify such breaks, we first smoothed out the time series using a moving average with a one-year sampling window, and rejected after or before the sudden change in the smoothed time series. After the quantitative cleaning, manual cleaning was performed on the remaining errors (isolated time series, erroneous oscillation, remaining sudden changes in soil moisture values).

TEXT-S1.2. Qualitative assessment of long-term trends

After the quantitative control, we qualitatively classified the soil moisture time series by visual inspection as (a) reliable, (b) unreliable, or (c) trending. Time series were categorized as '(a) reliable' if they comprised more than two seasonal cycles without apparent erroneous oscillation, fragments of data, implausible saturation, implausible sudden changes in soil moisture values, referring to Dorigo *et al.*, (2013); and categorized as '(b) unreliable' if not. The time series were categorized into '(c) trending' if the time series was reliable but had an increasing or decreasing trend in mean soil moisture value over the entire observation period, which can be caused by changes in the sensor voltage power (Rosenbaum *et al.*, 2012; Martini *et al.*, 2015), oxidation of sensor rods, salinization, soil compaction (Dorigo *et al.*, 2013). '(b) unreliable' and '(c) trending' time series were removed from the analysis. Only '(a) reliable' time series were used for this thesis because distribution type, estimated field capacity, and estimated wilting point were sensitive to the trending time series. Event-based and season-based signatures may be less sensitive to trends and could be calculated for both '(a) reliable' and '(c) trending' time series in future analysis.

FIGURE S1 Signature profile with soil depths between land-uses. In each study site, signatures from different sensor depths for a given land-use were compared. The upward, downward, and horizontal arrows indicate if the signature values were increasing, decreasing, or similar as soil depth increases for a given land-use. The cells are highlighted with colors associated with the p-value of the Kruskal–Wallis test. The cells are white when the sample size was not enough for the Kruskal-Wallis test (less than five). The frame lines of the cells are highlighted yellow if the signature profile with soil depth changed between land-uses

		Signatures										
		Event-based				Season-based				Timeseries-based		
						Dry-to-wet transition		Wet-to-dry transition				
Study site	Land-use (undisturbed disturbed)	Amplitude	Rising time	Rising limb density	No response rate	Start Day	Duration	Start Day	Duration	Estimated field capacity	Estimated wilting point	Distribution type (Unimodal)
WB	Forested	→	→	↗	↗	→	↘	→	↗	↘	→	↗
	Deforested	→	→	→	↗	↘	↘	↘	↘	↘	→	→
HB	Greenspace	↘	↗	↘	↗	↗	↘	↗	↗	→	→	↘
	Urban	↘	↗	↘	↗	↗	↘	↗	↗	↘	↘	↘
RM	Deep GW	↘	↗	↘	↗	↗	→	↗	→	↗	→	→
	Shallow GW	↘	↗	↘	↗	↗	→	↗	↗	↗	→	↗
TX	Ungrazed	↘	↗	↘	↗	↗	↘	→	↗	↗	↗	↘
	Grazed	↘	↗	↘	↗	↗	→	→	↗	↗	↗	↘
MQ	Non-wetland	↘	↗	↘	↗	↗	↘	↗	↗	↘	↗	↗
	Wetland	↘	↗	↘	↗	↘	↗	↗	↘	↘	↗	↗
OZ	Grass	↘	↗	↘	↗	↗	↘	↗	↗	↗	↗	-
	Grazed	↘	↗	↘	↗	↗	↘	↗	↗	↗	↗	↘
	Crop	↘	↗	↘	↗	→	↗	→	↗	↗	↗	↗

0 0.05 0.1 ≥ 0.15

P-value color scale

FIGURE S2 Box and bubble plots of all study sites for event-based signatures. The box is drawn between the first and third quartile, with a line in between indicating the median. The whiskers extend within a distance to the box equal to 1.5 times the interquartile range. Dots indicate the outliers

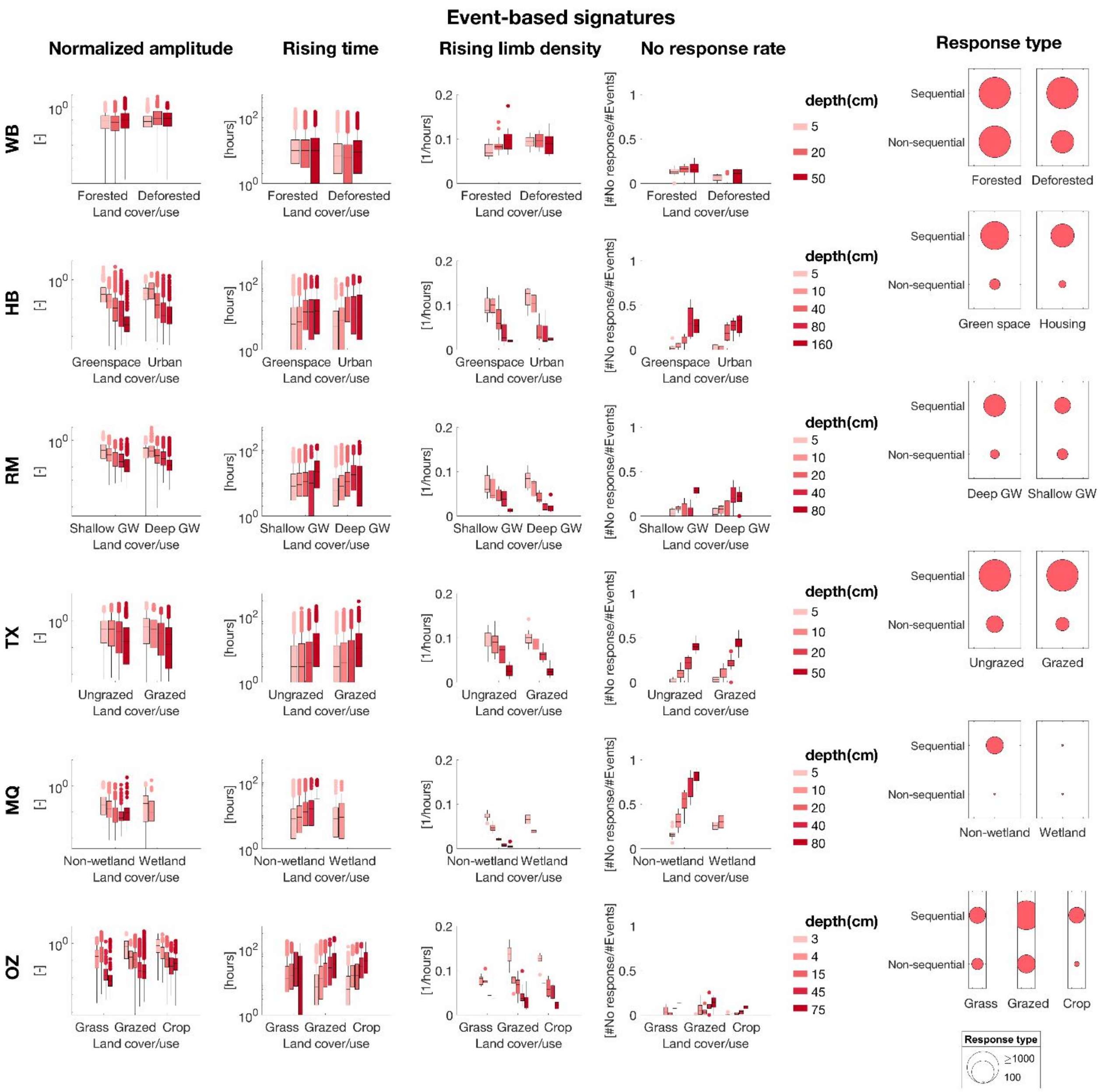

FIGURE S3 Box plots of all study sites for season-based signatures. The box is drawn between the first and third quartile, with a line in between indicating the median. The whiskers extend within a distance to the box equal to 1.5 times the interquartile range. Dots indicate the outliers

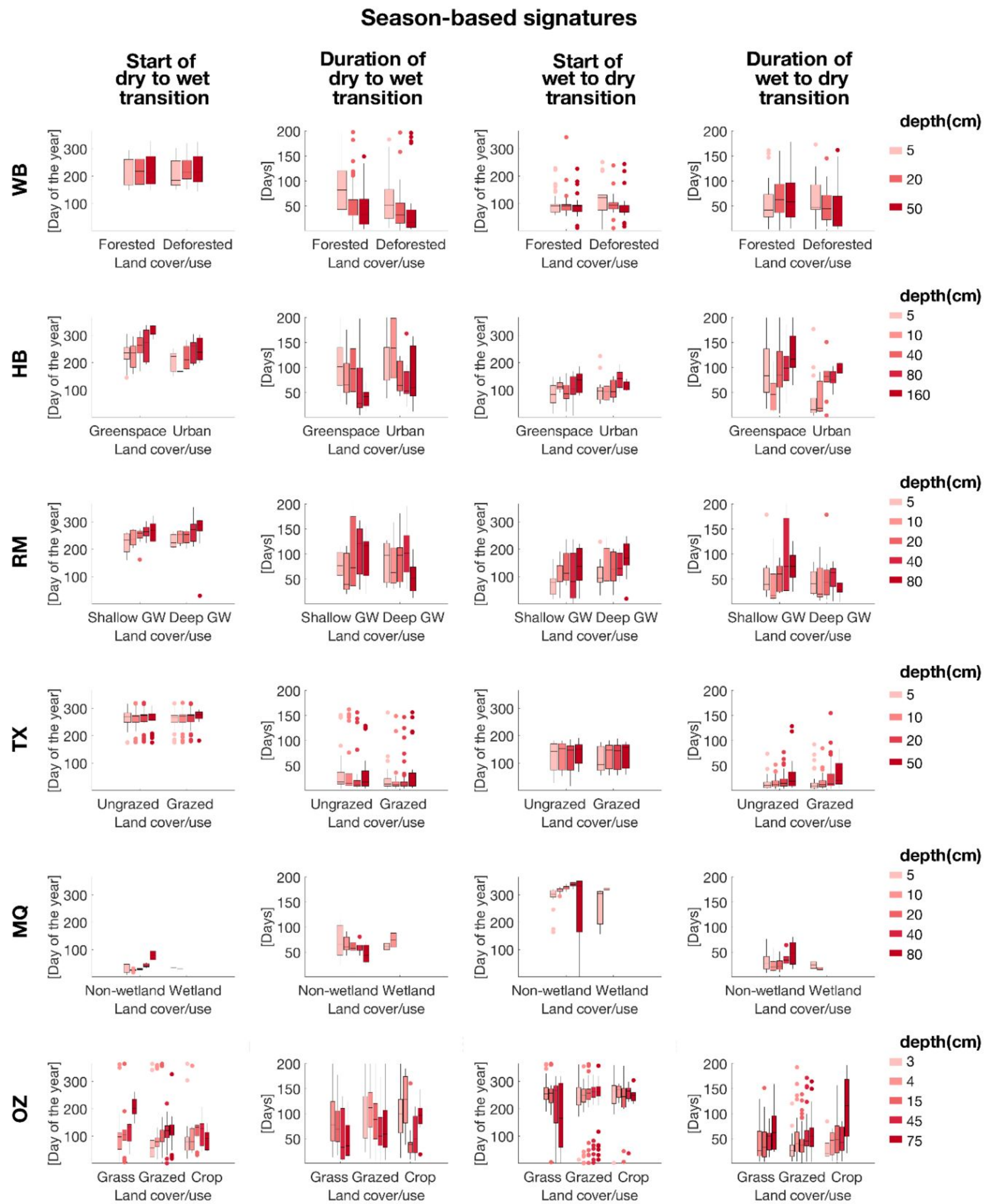

FIGURE S4 Box and bubble plots of all study sites for timeseries-based signatures. The box is drawn between the first and third quartile, with a line in between indicating the median. The whiskers extend within a distance to the box equal to 1.5 times the interquartile range. Dots indicate the outliers

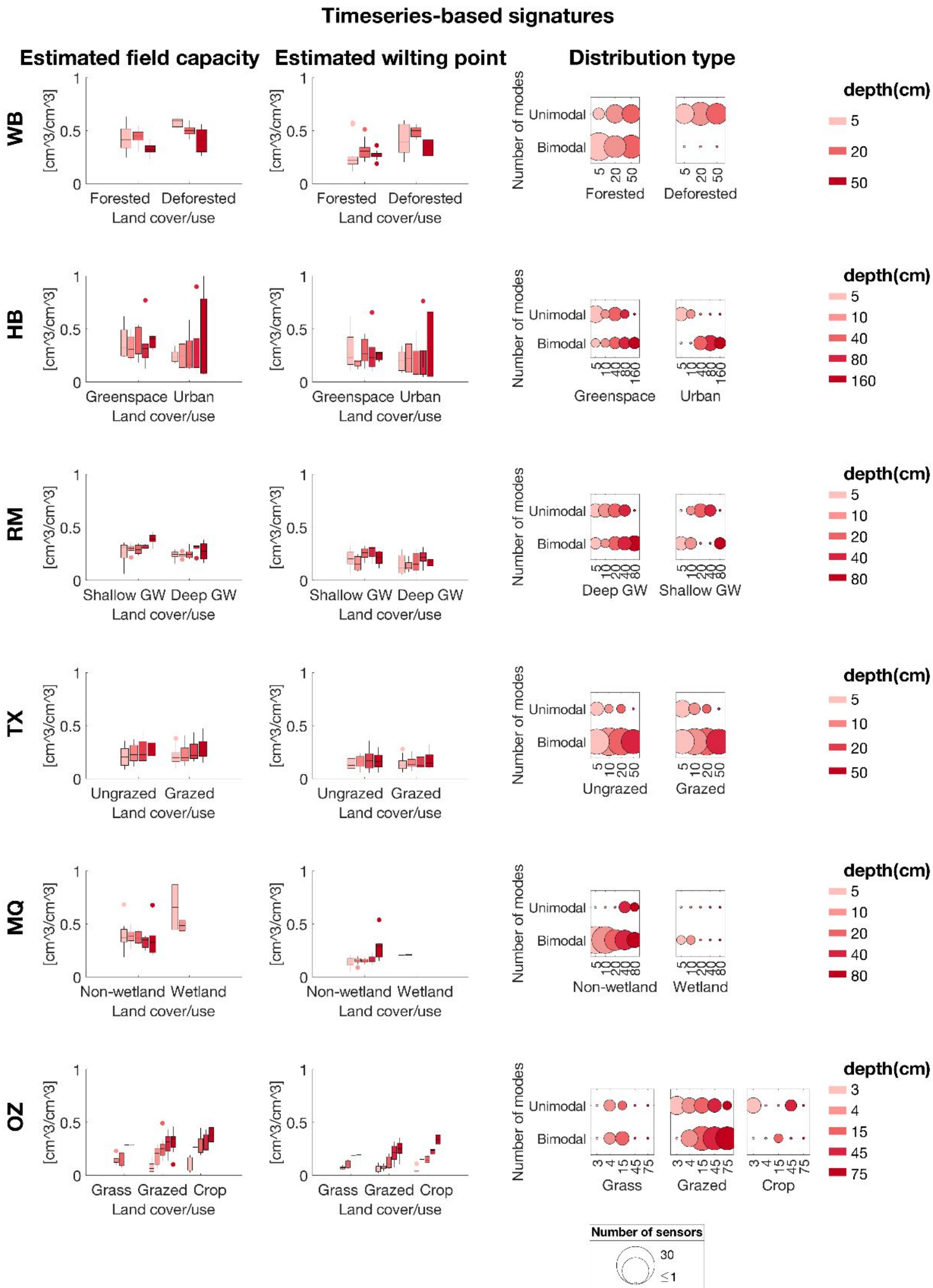

TEXT S2 Applicability of signatures to data from a wider variety of environments

Most soil moisture signatures were originally created and tested in limited environments. Since we applied those signatures to data from a broader range of environments, we encountered several difficulties extracting and interpreting the signature values. After visual inspection of time series and the graphical display of signature results, we summarized our recommendations below. We included those signature values in our results with careful attention.

First, extraction of seasonal signatures (timing and duration of seasonal changes) failed when there were two rainfall seasons. Since the seasonal transition signatures assumed only one wet season per year (Oznet site, OZ in Figure S5), the seasonal transition models did not fit the time series of data with two rainfall seasons (Texas site, TX in Figure S5). Another condition where season-based signatures failed was when freeze and thaw occurred (Maqu site, MQ in Figure S5). Seasonal transition signatures were initially designed to represent wet-to-dry/dry-to-wet season transition (Branger and McMillan, 2020); instead, they also represented freeze and thaw processes (Chen *et al.*, 2019; Wang *et al.*, 2019).

Second, the 'bimodal type' in distribution type signatures represented more than one sort of dynamics. The bimodal distribution was initially designed to represent soil moisture seasonality (Branger and McMillan, 2020). For example, weak seasonality in a station in Wüstebach (WB in Figure S5) was represented by unimodal distribution, and strong seasonality in a station in Oznet (OZ in Figure S5) was represented by bimodal distribution. However, bimodality also occurred in our data when there were large dry-downs (Texas site) even during wet seasons, or freeze and thaw processes (Maqu site).

Third, the degree of data quality control impacts the signature calculation. For example, the estimated wilting point signature did not give reliable values while the soil was frozen (Maqu site). This was because the sensors measure the electronic conductivity of ice once freezing starts (Dente *et al.*, 2012). Many studies reject soil moisture time series during freezing conditions as part of the quality control process. Nevertheless, the estimated wilting point was still helpful for calculating other signatures, such as normalizing the response amplitude, or constraining parameters when running seasonal transition signature codes. In this case, we recommend rejecting timeseries during freezing conditions only when necessary, such as not using estimated wilting point values for physical interpretation or calculating event-based responses. More generally, we recommend reviewing data quality control practiced by other literature (e.g., Dorigo *et al.*, 2013; Rosenbaum *et al.*, 2018) and visually inspecting the data and signature results.

FIGURE S5 A figure showing how the time series of data under diverse types of climates are translated into distribution type signature

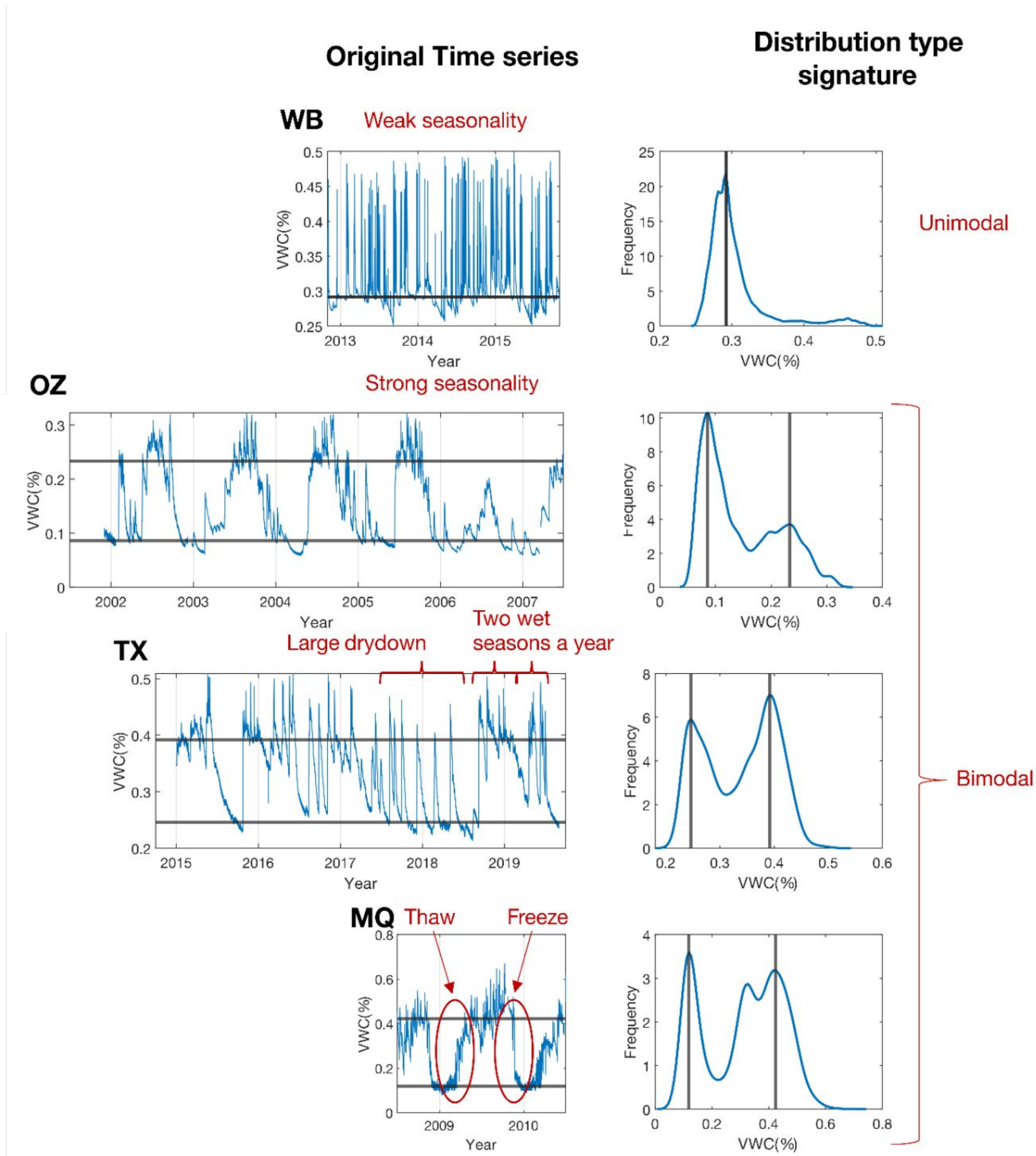

TABLE S1 Sensor configurations of the study sites. Data were derived from 'Key reference papers' cited in Table 1

Soil moisture network (name and abbreviation)	Network size (km^2)	Soil moisture measurement instrumentation (type of the sensor, manufacturer, product number, and the measurement accuracy reported by manufacturer)	Soil moisture sensor depth (cm)	Number of the soil moisture sensors	Observation record (length and period)	Rainfall measurement instrumentation (type of the sensor, and installation location)
Wüstebach WB	0.27	Capacitance sensors; Meter group; ECHO-EC5; ±3%	5, 20, 50	51	6 years, 2013 – 2018	Weight-based gauge; a national weather station located 8 km west of the catchment
Hamburg HB	755	6 stations in both land-uses: water content reflectometer; Campbell Scientific; CS616; ±2.5% 4 stations in both land-uses: capacitance sensor; Meter group; 5TM; ±2%	5, 10, 40, 80, 160	15	7 years, 2010 – 2016	Weight-based gauge; a national weather station located 8 km north of the catchment
Raam RM	223	Capacitance sensors; Meter group; EC-TM; ±3%	5, 10, 20, 40, 80	15	3 years, 2016 – 2019	N/A; a national weather station located within the catchment
Texas TX	1,296 Estimated as the area of 36 km square	Water content reflectometer; Campbell Scientific; CS655; ±1%	5, 10, 20, 50	38	5 years, 2014 – 2019	Tipping bucket gauge; at each soil moisture sensor location
Maqu MQ	3,200	Capacitance sensors; Meter group; EC-TM; ±3%	5, 10, 20, 40, 80	20	2 years, 2008 – 2010	N/A; a station next to a soil moisture sensor CST01
Oznet OZ	82,000 3 catchments with areas 145 km^2, 600 km^2, and 2,500 km^2	Sensors installed at 3 cm depth: soil dielectric sensors; Stevens Water Monitoring Systems; Hydraprobe; ±1% Sensors installed below 4 cm depth: water content reflectometer; Campbell Scientific; CS615 and CS616; ±2.5%	3, 4, 15, 45, 75	38	19 years, 2001 – 2019	Tipping bucket gauge; at each soil moisture sensor location